ADVANCED ‘GREEN’ COMPOSITES BASED ON AGRICUTURAL BY-PRODUCTS

A Thesis

Presented to the Faculty of the Graduate School

of Cornell University

In Partial Fulfillment of the Requirements for the Degree of

Master of Science

by

Denghao Fu

May 2020

ABSTRACT

Concerns regarding environmental deterioration as well as issues regarding the sustainability of fast depleting petroleum resources used to make conventional plastics have forced the scientific community to focus on developing and manufacturing new and novel 'green' materials that are fully biodegradable and derived from renewable, plant-based resources. In the present study a non-edible starch, extracted from avocado (*Persea americana*) seed starch (AVS), a waste product of avocado processing, was developed for fabricating 'green' composites. AVS was crosslinked using a green crosslinker, 1,2,3,4-butane tetracarboxylic acid (BTCA), and a catalyst, sodium hypophosphite (SHP), to prepare a rigid thermoset resin with improved water resistance. Two cellulose based reinforcements, micro-fibrillated cellulose (MFC) with average diameter of 50 nm and velvet leaf (a common weed) stem derived microfibers (VLF) with average diameters of 12 μm were used to fabricate green composites. Properties of these green composites were fully characterized and compared with different compositions. In addition, advanced 'green' composites with excellent mechanical properties were fabricated by combining liquid crystalline cellulose (LCC) fibers with MFC blended AVS (MFC/AVS) resin. LCC fibers were modified using a combination of alkali and heat treatments to further improve their tensile strength from 1.5 GPa to over 1.9 GPa. The advanced green composites prepared by simple hand layup showed average tensile strength of 380 MPa and Young's modulus of 25 GPa with only 40% of LCC fibers by volume. This study clearly demonstrates the potential of AVS based green composites for industrial applications such as automotive, packaging, construction and others.

BIOGRAPHICAL SKETCH

Denghao Fu was born in China on 26th March, 1996. He received his bachelor of engineering (B.S.) degree in Polymer Materials and Engineering from South China University of Technology, Guangzhou, China in 2017. In September 2017, he joined Dr. Netravali's group at Cornell University, Ithaca, NY, to earn his Master of Science (M.S.) degree in Materials Science and Engineering and focused on 'Green composites' based on natural resources. He is currently pursuing Doctor of Philosophy (Ph.D.) in Materials Science program in Michigan State University in East Lansing, MI, focusing on photopolymerization, dental adhesive and bio-active composites.

Dedicated to my Family and Friends

ACKNOWLEDGMENTS

I would first like to thank my thesis advisor Prof. Netravali for his support, encouragement and patience. He consistently steered me in the right direction for both research and academic writing. I feel fortunate to receive his guidance to be a qualified scientific researcher.

I would also like to acknowledge Cornell Center for Materials Research (CCMR) and both the Department of Materials Science and Engineering and Department of Fiber Science & Apparel Design.

Finally, I would like to thank Prof. Eve Donnelly, Prof. Sue Watkins, my colleagues, Namrata, Anusha and Shanshan, and my family for their support.

TABLE OF CONTENT

LIST OF FIGURES

LIST OF TABLES

CHAPTER 1: INTRODUCTION

1.1 Green biodegradable composites

Composites are made by combining two or more different components to obtain desired properties. Different components may be combined in different proportions and organized differently to obtain various structures and desired properties. They not only retain the merits of each component, but also obtain integrated properties with the combination of each constituent through synergistic interactions.[1] Composite materials normally consist of reinforcements that include micro- and/or nano- particles or fibers, and a binding agent termed as matrix or resin in the form of polymer, ceramic or metal. The definition of composite materials was first put forward when glass fiber reinforced plastic was invented for use in aerospace industry in the 1950s.[2] After that, carbon, boron, silicon carbide and aramid fibers, silica nanoparticles, carbon nanotubes and graphene sheets were synthesized and have been combined with different types of resins such as synthetic epoxy, rubber, ceramic and metals such as aluminum and titanium for use in diverse applications including construction, aerospace and automotive applications.[3]

As one of the most common composites, fiber reinforced polymer composites have been commonly used for decades in many structural applications due to their light weight, high strength and stiffness as well as the ability to engineer the properties in different directions.[4] For the fiber part, most common fibers include glass, carbon and polymeric fibers such as Kevlar® and ultrahigh molecular weight polyethylene. Common polymeric resins include thermoplastic polymers such as polypropylene (PP), polyethylene (PE), polyvinyl chloride (PVC) or thermoset polymers such as epoxy and polyurethanes (PU). The resins play an important role to hold the fibers in their respective positions and transfer the load from broken fibers to intact fibers through the fiber/resin

interface.[5] As a result, besides the respective mechanical properties of fibers and resin, the adhesion at the fiber/resin interface is of critical importance in composites to obtain desired properties. Adhesive bonding between fiber and resin should be strong enough to avoid debonding and resulting in fiber pulling-out from the resin during composite fracture.[6]

With the rapid development and improvement of tougher, stronger and multifunctional advanced composites, their use in diverse applications has increased many folds in the past 4-5 decades. Most of the fibers and resins mentioned above do not degrade in normal environments. With large amounts of composites being produced and used, disposal at the end of their life has become a serious problem. In 2018, the U.S. glass fiber consumption reached 2.5 billion pounds and at the same time worldwide carbon fiber consumption increased to 75,000 metric tons.[7] To figure out the waste disposal problem, some recycling techniques have been developed including thermal recycling, chemical and mechanical recycling.[8] However, recycling costs, lower quality of recycled materials and the technical barrier posed by the complexity of different composites still hinder the development of composite recycling process.

Concerns regarding environmental degradation and sustainability of resources, in recent years, have forced the scientific community to develop and manufacture bio-based composites or 'green' composites that are both biodegradable and derived from renewable resources.[9] The development of green composites offers an opportunity to cut down the utilization of synthetic polymers derived from petroleum and ease the pressure of composite waste disposal. The recent successes of green composites have helped government and corporations to further focus on these and newer sustainable materials.

For the fiber reinforcement of green composites, lignocellulosic fibers such as hemp,[10,11] sisal,[12] flax,[13] kenaf[14] are believed to be good alternatives to replace traditional synthetic fibers. Although

the natural cellulosic fibers are not as strong or stiff as synthetic fibers such as Kevlar® or carbon fibers and have some weaknesses that include higher water absorption and thermal expansion, crystalline cellulose materials with their high intrinsic strength could still satisfy the demand in many fields including semi-structural and infrastructure and in some cases structural applications as well.

For the resin part, in recent years, researchers have been trying to use degradable materials and replace conventional polymers to create fully degradable composites. Some biodegradable synthetic polymers including poly(lactic acid) (PLA), poly(3-hydroxybutyrate-co-3-hydroxyvalerate) (PHBV) and polybutylene succinate (PBS) have already proved to have comparable mechanical properties with those of PE and PP.[15] However, the cost of synthesizing these biodegradable polymers might prove to be a barrier for large-scale manufacturing. Also, the reliance on raw materials from specific sources for polymer synthesis and low degradation rate compared with natural materials, are other limitations to develop these types of synthetic biodegradable materials.[15]

Another group of materials, bio-based materials obtained from natural sources, mostly plants, including starch, protein, chitosan, cellulose and lignin, have attracted research community's attention because of their lower cost and better biodegradability. This has prompted using these sustainable materials in many applications and made it easier to move away from petroleum-based ones.

The term 'Fully green composite', means that both resins and reinforcing agents are biodegradable and mostly made from renewable natural resources, e.g., plants.[9] Also, at the end of their useful life, green composites can be easily composted rather than being dumped in landfills. Such green composites are most favorable from an environmental protection point of view and are

considered be a sustainable substitution for the traditional nondegradable petroleum-derived composites.[9]

1.2 Sustainability and practicability of green composites

Application of green composites has rapidly increased in the last decade in many fields including aerospace, automotive, food packaging and some structural applications, although the overall use is still low.[16,17] For example, in transportation application, green composites can be used in many car components including door and floor panels. In 2017, International Automotive Components Group (IAC) put forward the first natural fiber composites sun-roof frame made from hemp and kenaf. It not only met the mechanical requirements of the vehicle but was believed to create significantly less air pollution and use less energy for manufacturing.[18] In addition, the lighter weight of the green composites can be expected to improve fuel efficiency and reduce greenhouse gas emissions.

Another application has been in architecture and building decorations.[9,13] The development of green composites can start a new revolution in green buildings, replacing the non-recyclable materials in roof panels, furniture, door liners and window frames.

Green composites combining natural fibers and bio-based materials have shown outstanding mechanical properties. However, to fully launch green composites commercially, several issues need to be resolved. First, the compatibility between cellulosic fibers and hydrophobic resins is comparably low. Some biodegradable polymers such as PBS and PLA are hydrophobic while natural cellulosic fibers are hydrophilic with high surface energy. This difference in chemical properties weakens the bonding between fibers and resin and reduces the composite properties.

Hydrophilic resins, such as most of the plant-derived green materials including starches, chitosan and proteins, have large number of hydroxyl groups leading to high moisture absorption. When water is absorbed by composites, the interface adhesion is weakened and the formation of voids and cracks are promoted, both causing the loss of mechanical properties.[19] Some other disadvantages such as fast degradation through microbial attack and not-yet-mature manufacturing technology, have also become barriers for increasing commercial practicability and viability of green composites.

In the present research, fully biodegradable green composites with good mechanical properties were fabricated. Starch from an agro-waste source was reinforced by both nano- and micro-scale cellulose termed microfibrillated cellulose (MFC) or micro-scale cellulose extracted from a commonly found weed. Starch, for resin, was extracted from avocado (*Persea americana*) seeds, by-product of food processing, which are typically discarded.[20–22] The microfibers were extracted from the weed, velvet leaf (*Abutilon theophrasti*), by using a combination of mechanical pulping and chemical treatment.[23] To solve the issues related to water absorption and low mechanical properties, avocado seed starch (AVS) was crosslinked using a green crosslinker, BTCA, to form a thermoset resin.[24,25] Chemical compositions, thermal and mechanical properties of MFC reinforced composites (MFC/AVS) and velvet leaf microfiber based composites (VLF/AVS) were fully characterized.

Finally, in order to fabricate 'advanced green composites' with high mechanical properties, liquid crystalline cellulose (LCC) fibers were used as the primary reinforcement with MFC/AVS as the resin. Further, LCC fibers were modified (M-LCC) by treating them in alkali solution under tension as well as thermal treatment to improve their properties further. Both LCC and M-LCC fibers were then used, separately, to fabricate green composites with high strength. The resin 30:70

blend of MFC/AVS, was further crosslinked using BTCA. Fabrication of unidirectional green composites involved aligning LCC yarns with predetermined layers in MFC/AVS resin using simple hand lay-up, drying and compression molding. The effect of plasticizer (sorbitol or glycerol) addition in the resin were also investigated. The results showed excellent mechanical properties of LCC-reinforced MFC/AVS advanced green composites that could be used in primary structural applications in construction, automobile and other areas.

CHAPTER 2: LITERATURE REVIEW

2.1 Starch based resin

2.1.1 Starch-based plastics

As a bio-based polymer, starch is considered to be environmentally friendly because of its low or zero greenhouse gas emissions. It is one of the favored resins for green composite fabrication where the biodegradability and non-dependence on petroleum are desirable. Figure 1 shows the global production capacities of bioplastics in 2019.[26] As can be seen in Figure 1, it has been estimated that about 2.1 million tons of bioplastics were globally manufactured in 2019 and almost 21.3% of them were starch-based.[26] Same report also predicted that starch-based plastics will continue to grow and be used more in diverse fields including flexible packing, medical treatment, construction and electronic devices.[26]

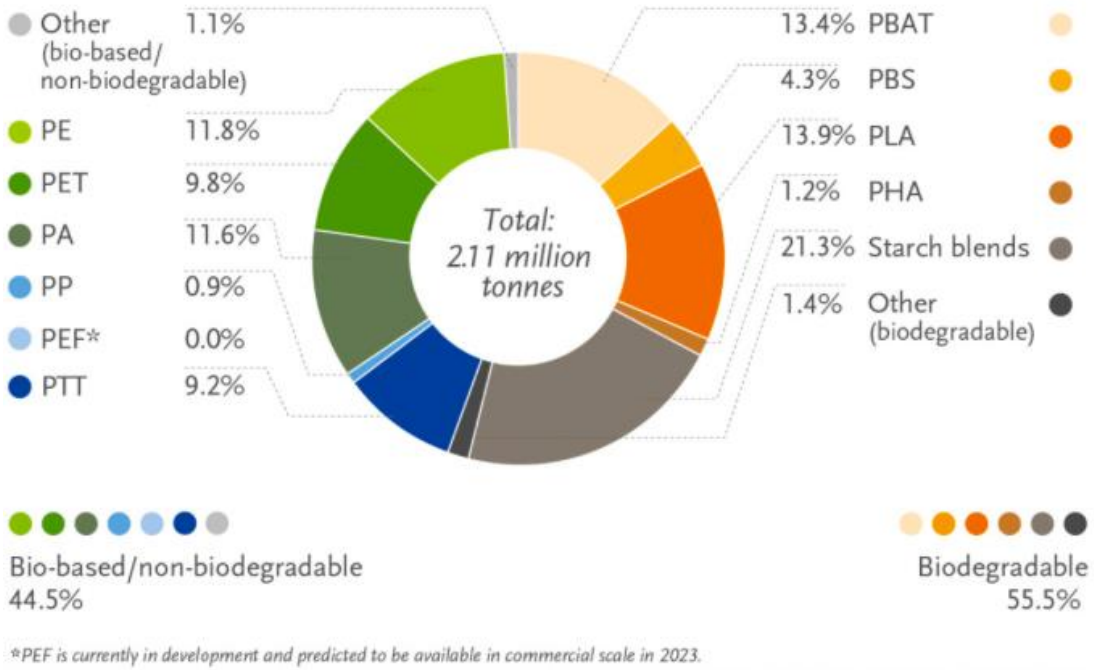

Fig. 1 Global production capacities of bioplastics in 2019 [26]

2.1.2 Chemical structure of starch

Starch is one of the most common food sources in our society. It is most produced and preserved in many parts of plants especially in roots, fruits and seeds as energy storage. Among all plants, rice, maize, potato, cassava, wheat are the most common sources for starch. Starch exists in the form of granules with sizes ranging from 2 μm to 100 μm.

Starch is made by combining glucose repeat units. There are mainly two types of molecules within starch, linear amylose and branched amylopectin as shown in Figure 2.[27] Amylose is a linear molecule with (1-4)-α-linkage with average molecular weight ranging from 10^5 to 10^6. It exists in a helix form and has no branches. Compared to amylose, amylopectin molecules are highly branched with relatively high molecular weight between 10^6 to 10^7 g/mol and exist in double

helical structure. Glucose units in amylopectin can both be bonded with α-(1-6) or α-(1-4) linkages. As a highly branched structure, amylopectin exists predominantly in crystalline form.[27]

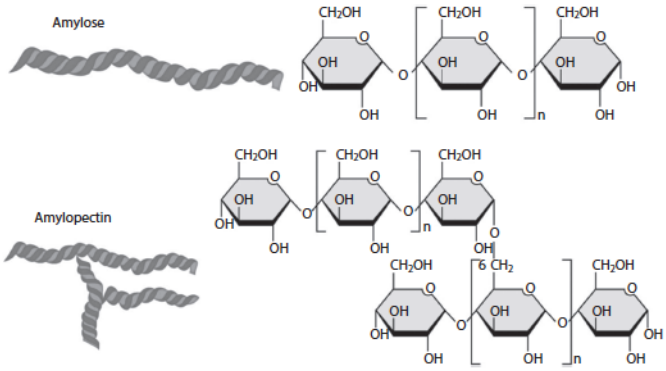

Fig. 2 Structure of amylose and amylopectin molecules [27]

The proportion of amylose and amylopectin varies in different plants, with generally 20%~30% of amylose and 70%~80% of amylopectin. The different proportions of amylose and amylopectin give rise to various structures and properties to starch.

2.1.3 Modification of starch-based materials

In spite of the inherent advantages and increasing demand of starch-based plastics, several challenges still need to be addressed before large scale production of starch-based composites can be possible. First, pure starch has very low mechanical properties which makes it difficult to process.[28] Second, the hydroxyl groups present in starch-based materials allow them to readily absorb moisture which lowers their fracture stress as well as glass transition temperature (T_g). Most plasticizers used for starches are themselves hydrophilic and their addition further increases the moisture absorption and lowers strength and T_g even further.[29] To overcome these problems, some modifications such as physical blending with reinforcing particles or fibers/fibrils, chemical

modifications including crosslinking, esterification and graft copolymerization, etc., have been developed during last couple of decades. Each modification will be mentioned below.[28–44]

1. Plasticizer

Pure starch resins are very brittle, difficult to bend and very weak. However, when plasticizers such as glycerol or sorbitol are added to starch, the strong intermolecular hydrogen bonding is disrupted. In addition, the large amount of free volume brought in by the plasticizers results in lower T_g and significantly higher flexibility for the starch-based materials. This allows raw starch to be processed as thermoplastic starch (TPS).[37,38,45] Although high flexibility and fracture strain of TPS are obtained, it still has low mechanical properties (1~10 MPa fracture stress and over 100% fracture strain)[10,28,37,39–41,45] compared to traditional polymers such as PE (14~40 MPa fracture stress and over 100% fracture strain),[5] PP (26~41 MPa fracture stress and over 100% fracture strain),[5] PLA (60 MPa fracture stress and 3.5% fracture strain),[42,46] and PBS (27 MPa fracture stress and 16% fracture strain).[47] As a result, other modifications have to be done to make the application of starch-based composites feasible.

2. Blending with other polymer and reinforcements

One of the most common physical modifications is blending with hydrophobic materials. Starch had been blended with other biodegradable polymers including PLA, PCL, etc.[42] Synthetic biodegradable polymers normally have higher cost but excellent mechanical properties and water stability. As a result, the proportion of the synthetic polymer/starch blend could be adjusted to reach the requirements of low cost, high mechanical properties as well as water stability. Compatibilizers, such as maleic anhydride (MA) are generally needed to improve the compatibility between starch and other hydrophobic synthetic degradable polymers.[42]

Besides blending with synthetic polymers, starch-based plastics can also be blended with reinforcements to further improve their strength, modulus (stiffness) and decrease their water absorption. Common reinforcing agents include rigid particles and fibrous materials. Rigid particles such as montmorillonite,[39,40] fly ash,[41] chitosan,[43] and other metal particles,[44] can be well controlled to disperse uniformly in starch resins. The particle size, however, should be strictly controlled to avoid defect formation and stress concentration. Fibrous materials are by far the most common reinforcing agents. Within biodegradable materials, cellulose fibers have high specific stiffness and can hydrogen-bond well with starch-based materials because of their chemical similarity. Review of cellulose fiber reinforced composites will be covered in section 2.2.

3. Chemical treatments

Besides physical blending, several chemical modifications of various starches have also been studied for many decades.[30–36] Starch grafted copolymerization, esterification and crosslinking are some of the common chemical methods which reduce the exposure of hydroxyl group of starch molecules and, thus, address the inherent hydrophilicity related problems of starch. Each glucose unit in starch has three hydroxyl groups. One of them is a primary group and the other two are secondary hydroxyl groups. The primary groups are much more reactive than the other two and are more amenable for chemical modifications. As a result, most chemical modifications to transform cellulose into different structures involve the primary groups.[30]

Starch grafted copolymers were obtained by chemically bonding starch molecules to other synthetic polymers, such as starch-g-methacrylamide, starch-g-methacrylonitrile, starch-g-polyvinyl alcohol, starch-g-polystyrene.[31] After grafting with other polymers, thermal stability, mechanical properties and film processing properties have been shown to improve.[31] Starch esterification has also been a common chemical modification. In this case hydroxyl groups were

substituted with hydrophobic functional groups to form starch acetate or starch hydroxypropylate.[30] Presence of less number of hydroxyl groups equates to better water stability.

Another solution to overcome these weaknesses is to crosslink them into thermoset starches. Crosslinked starch is synthesized through reacting some of the primary hydroxyl groups in starch with other small bi- or multi-functional molecules containing carboxylic, aldehyde, phosphate and phosphoryl chloride groups, to obtain 3-D network structures.[24,32–36,48] A variety of crosslinking agents have been used for modifying various starches (corn, rice, tapioca, etc.) including epichlorohydrin (EPI),[32] sodium trimetaphosphate (STMP) and phosphoryl chloride (POCl).[33] In recent years, greener crosslinkers including polycarboxylic acids such as malonic acid,[34] citric acid,[35] 1,2,3,4-butane tetracarboxylic acid (BTCA),[24,25] and multi-aldehyde oxidized sucrose[36,48] have been introduced. Chemical structures of some common 'green' crosslinkers are presented in Figure 3. After crosslinking, the fracture strains of starches have been shown to reduce to between 2 and 30% depending on the amount of plasticizers used.[24,25,34–36] However, other properties including tensile strength, Young's modulus and thermal, water and organic solvent stability improved significantly.[24,25,34–36]

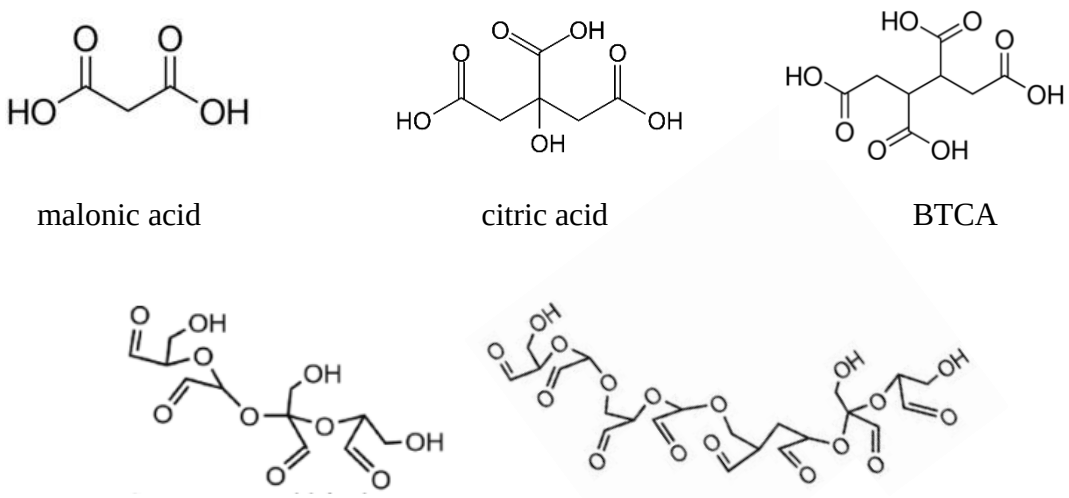

Fig. 3 Chemical structures of some common 'green' crosslinkers

2.1.4 Starch made from plant waste—avocado seed

Until now, starch-based composites have been considered to be good substitution for petroleum-based materials. Among all kinds of starch sources, corn,[49] potato,[49] cassava,[50,51] have been most used and most studied. However, since these starches are edible for humans and animals, questions have been raised about taking food away to make composites for construction or packaging. Indeed, this can hurt poor people the most. Non-edible starch, which does not impact the human daily diets would obviously be a better choice. Also, since most available non-edible starch sources are waste or unusable by-products, using them should not only be more sustainable but also solve the waste issues, making this a win-win solution. Studies on starch-based waste by-products have been already done on mango seeds,[24,52,53] jackfruit seeds,[54] horse chestnut[55], etc. For example, horse chestnut starch was extracted to make thermoplastic starch by melt blending with glycerol. However, the mechanical properties were relatively low compared with other common starches with fracture stress of only 2~3 MPa and fracture strain of 1%.[55] Lubis, et al.,[54] used jackfruit seeds

to extract starch and blend with 20 wt% chitosan and obtained strength of 13.5 MPa. Patil and Netravali,[24,52] created bio-plastics from mango seed kernel starch with 16 MPa fracture stress after crosslinking with BTCA. Higher fracture stress of 50 MPa was obtained by reinforcing it with 40 wt% microfibrillated cellulose (MFC).[52]

As another kind of waste by-product, avocado (*Persea americana*) seeds have been studied for their chemical structure. Starch content in fresh avocado seed (AVS) is around 30% by weight, and the seeds are around 16% of the total fruit weight.[56] It is, thus, promising to extract the non-edible starch from avocado seeds on large scale to substitute conventional edible starches such as corn and rice.

Avocado originated in Mexico and central America and are now widely grown in California. They are also commonly grown in other tropical and subtropical regions of the world. Because of its high content of monounsaturated fat, avocado has become an important food source to replace other fatty foods including meat in vegetarian diet. They are also used in oil extraction, seasoning and desserts. In 2014, world production of avocado was recorded at 5.0 million tones.[57] The avocado production and processing industry has rapidly developed not just in food products, but has diversified in cosmetics and pharmaceutical industries.

AVS has been recently used to fabricate green composites. Ginting, et al.,[21] obtained AVS composite films with highest fracture stress of 30.2 MPa and Young's modulus of 2031 MPa after adding 40 wt% chitosan. The fracture strain, however, was lower than 2%. The highest fracture strain of 5.4% was obtained after adding 10% chitosan, while strength and Young's modulus were only about 10 MPa and 200 MPa, respectively. As for fabricating green composites using AVS as resin, a trade-off may be reached between high strength and high fracture strain, depending on the application.

2.2 Reinforcement using cellulose-based fibers

2.2.1 Chemical structure of cellulose

To make fully green biodegradable composites, reinforcements used should not only provide excellent mechanical properties but should also be fully biodegradable. As the most common bio-based biodegradable polymer, cellulose meets both these criteria. Cellulose is a linear chain polysaccharide with D-glucose units linked with β 1→4 bond, which is different from the α 1→4 link of amylose in starch.[27] Compared with amylose, the glucose repeat units in cellulose are rotated 180^{o} for each successive glucose. The bonds limit the free rotation of C-O-C (ether) bond which gives the structure higher stiffness and strength.[27] Also, β 1→4 bonds allow the formation of stronger intermolecular hydrogen bonds resulting in high stiffness of cellulose molecules.

The cellulose I crystal structure have super high axial modulus about 138 GPa and specific strength of 667 MPa·cm^{-3}·g^{-1}, which are even much higher than glass fiber and close to Kevlar.[58] In nature, plant cell wall can be considered as a composite consisting of cellulose I as the reinforcing phase and amorphous cellulose-lignin-hemicellulose as the resin phase. Cellulose in plants has a hierarchical structure from microscale structure including cell wall, fiber cluster with hemicellulose and lignin, to nanoscale structure like nanofibrils, and even molecular structure including glucose β 1→4 links and hydrogen bonding.[17,27]

2.2.2 Cellulose-based microfibers and nanofibers

1. Cellulose-based microfibers

Plant derived cellulose fibers have become popular in many applications because of their low density, biodegradability and excellent specific mechanical properties.[59–61] Many plant fibers including hemp,[10,11] jute,[49] sisal,[12] flax,[13] ramie,[62] coconut,[63] pineapple leaf,[64] kenaf,[14] etc., have

been already used for polymer reinforcements. These fibers have been aptly called lignocellulosic fibers because most of them contain both hemicellulose and lignin along with cellulose. Although lignin and hemicellulose in cell wall serve to hold cellulose molecules and provide mechanical properties to plants, in fabricating composites, lignin and hemicellulose can lower the mechanical properties by weakening the interfacial fiber/resin adhesion. As a result, these components are commonly removed by alkali treatment. Alkali treatment is the most common process used for natural fibers such as cotton and is known as mercerization.[12] NaOH or KOH solution could be used to remove the lignin, wax and hemicellulose in order to increase the crystallinity of fibers.[12]Also, because of the removal of lignin and hemicellulose, increased fiber surface roughness can be achieved which, in turn can provide large surface area and better fiber/resin interaction.

Traditional plant fibers such as flax, bamboo, cotton, sisal have been already studied because of their high fiber content and plentiful availability. Other fiber sources, especially from agricultural wastes, including pineapple leaves, coconut husks and straw stalk have also been widely studied to fulfill the 'green economy' and avoid pollution.[65] However, there are many other waste sources that remain to be explored. Velvet leaf (*Abutilon therophrasti*) is one of the high cellulose content plants and is regarded as an agricultural weed. This plant, however, can be fully used because of the good fiber quality as a substitute for other traditional fiber sources. Reddy and Yang,[23] have already used alkali treatment to extract velvet leaf long fibers and their mechanical properties were found to be even better than kenaf, though the crystallinity was comparably low because some non-cellulose component remained in the fibers. The average single fiber diameter was 11.4 μm according to Reddy and Yang, which is smaller than fibers obtained from other common cellulose

sources.[23] This fiber source is promising as a substitution of the common cellulose sources to further reduce cost and utilize a waste source.

2. Cellulose-based nanofibers

Micro-cellulose fibers can also be converted into nanocellulose materials by mechanical processes including grinding,[66] ultrasonic treatment[67] and high pressure homogenization[68,69] that provide high shear stresses to isolate them into single nanofibrils. Common cellulose materials can be divided into cellulose nanofibrils and cellulose nanocrystals. Microfibrillated cellulose (MFC), which have fibrils from microscale to nanoscale, have much higher aspect ratio with average diameter of about 10~30 nm and length to microscale. The 3-D network-like or entangled structure of MFC not only has high crystallinity but also provides significantly larger surface area to interact with resin and provides improved dispersity of fibers within the resin.[69] Another nanocellulose material is cellulose nanocrystal. After strong acid hydrolysis, the C-O-C bonds of MFC are further broken, preferably in the amorphous parts and help turn cellulose nanofibers and microfibers into much shorter nanorods with lengths in the range of only hundreds of nanometers.[70]

While most nanocellulose products are primarily made from various wood pulps, CNC and MFC have also been extracted and extensively studied from other fibers from abundant plants such as hemp, kenaf,[69] bagasse,[71] bamboo, to agricultural by-product including coconut hulls, banana peels,[72] wheat or rice straw[73,74]. These nanocellulose materials from by-product sources not only provide similar properties when reinforcing polymer resin but also make full use of plant wastes. Bacterial cellulose (BC), secreted by bacteria such as *acetobacter xylinum*, is also a type of cellulose nanofiber.[75,76] BC have high purity of cellulose and smaller diameter rather than MFC. Typical, BC have higher reinforcement properties than plant-based MFC.

2.2.3 Cellulose-based fully biodegradable green composites

1. Green composites based on cellulose microfibers

There are three types of fiber composites according to the fiber orientation as shown in Figure 4.[3,77] Figure 4 (a) shows long fibers aligned or oriented longitudinally, in one direction. Since load can be transferred only in the longitudinal fiber direction, this orientation results in much higher tensile strength and Young's modulus in the fiber direction compared to transverse direction in which no contribution from fibers is expected. Figure 4 (b) shows short fibers in one direction called 'discontinuous alignment'. It is cheaper to fabricate but the reinforcement effect is lower than oriented composites. Figure 4 (c) shows random short fiber composites. The reinforcement in this case is lower than (a) and (b), but mechanical isotropic behaviors and high processability could be achieved. These composites can be easily processed using molding, compression or extrusion techniques.

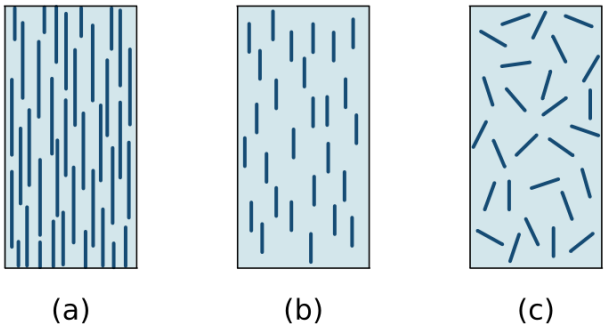

Fig. 4 Three types of fiber-reinforced composites [77]

Short microfibers from different sources have been used to reinforce thermoplastic starch (TPS).[37,45,49,76,78,79] In 1998, Wollerdorfer and Bader,[78] studied the influence of natural fibers on the mechanical properties of biodegradable polymers. By adding different amounts of flax

microfibers with the lengths varying from 100 to 1,000 μm, the tensile fracture stress increased from 8.91 MPa for pure TPS to 19.87, 26.23 and 36.42 MPa of composites with 10, 15 and 20 wt% flax microfibers, respectively.[78] Short winceyette microfiber (12 mm long) reinforced thermoplastic corn starch composites were investigated by Ma, et al.[79] Tensile strength significantly improved from 4 MPa to 15 MPa when the microfiber content increased from 0 to 20 wt%. The fracture strain, however, decreased from over 100% to around 20%.[79] Lodha and Netravali,[62] explained the effects of microfiber content and length by using interfacial shear strength tests. Short ramie fibers with lengths of 5, 10 and 15 mm were used in their study to reinforce soy protein. Critical length, from interfacial shear strength, was calculated to be 2.54 mm. Fibers with low weight content (loading) or having length lower than critical length would not improve the mechanical properties of soy protein resin. Instead, voids and flaws might be introduced into composites and even reduce the mechanical properties of composites.[62] By comparing different fiber content and length, it was found that these short fiber composites showed increased fracture stress and modulus with increase in fiber content from 0 to 30 wt% or as the fiber length increased from 5 mm to 15 mm. However, the fracture stress and Young's modulus of 30 wt% 15 mm microfiber were lower than the theoretical prediction because of the delamination failure due to fiber aggregation.[62]

In general, volume fraction of fibers to obtain maximum strength and Young's modulus depends on the manufacturing process, compatibility of resin and fibers, the respective mechanical properties and chemical structures of resins and fibers. Another critical parameter for microfiber reinforcement is their aspect ratio which is the length divided by the diameter (L/D). Higher aspect ratio, in general, provides better mechanical properties because of the less end stress concentration effect (fiber ends do not carry any load) and the larger surface areas for higher interfacial action

between resin and fibers.[62] However, fiber dispersion in resin might be affected because fibers are more likely to aggregate or entangle at high aspect ratios.

2. Green composites based on cellulose nanofibers

Because of the higher aspect ratio and surface area, cellulose nanofibers or microfibrillated cellulose (MFC) are thought to be better reinforcing agents than microfibers. During the past five years, more and more plant sources including hemp, sisal, banana peels, bamboo, have been used to extract nanofiber and used with different resins as reinforcement.[69–74]

Due to the innate hydrophilic behavior, cellulose nanofibers and MFC are widely used to reinforce hydrophilic resins such as various starches and proteins and synthetic polymers such as polyvinyl alcohol (PVA).[80–83] For example, MFC was blended with polyvinyl alcohol (PVA) to make degradable composites.[80] Results showed that MFC fibrils bonded well with PVA and dispersed uniformly even at a high loading of 50%. At this loading, composites showed excellent fracture stress in the range of 85 MPa and Young's modulus of nearly 4 GPa, which is much higher than many traditional polymers. Crosslinking can further improve the water and thermal stability.[80]

Materials from nature such as starches, proteins, chitosan, etc., are inherently hydrophilic and should be promising materials as resins to interact with hydrophilic nanoscale cellulose fibers. For example, soy protein isolate (SPI) was reinforced with MFC extracted from bamboo fibers. With only 30 wt% of MFC, fracture stress and Young's modulus improved from 20 (control) to 60 MPa, and from 0.6 GPa (control) to 1.8 GPa, respectively, without sacrificing too much fracture strain.[81] Starches have been also reinforced using micro- and nano-cellulose fiber. Ghosh Dastidar and Netravali combined MFC with waxy maize starch which contains high proportion of amylopectin of over 99%.[25] Their results showed that 15% of MFC could obtain tensile fracture stress of 39

MPa, fracture strain of 3.1% and Young's modulus of 2.3 GPa.[25] In order to avoid controversy of using food to make composites, Patil and Netravali used non-edible mango seed kernel starch as resin and crosslinked it with BTCA (40% by wt) to further increase the mechanical properties and lower the moisture absorption.[24] MFC loading of 40% resulted in tensile strength of 50 MPa and Young's modulus of 2.4 GPa.[52]

Other non-edible sources for resin, including Jatropha (Jatropha curcas) seed cake protein,[82] Neem (Azadirachta indica) seed cake protein,[83] Karanja (Pongamia pinnata) seed cake protein,[84] were also studied to fabricate composites by combining them with MFC. Crosslinkers were used in all these cases to react the amine groups in protein to enhance water stability and MFC were added to further raise their stiffness and strength.[81–84] Results from all these works based on waste sources of proteins and starches showed comparable results with those made using traditional food sources. This shows that these waste residues can be potential materials for composite fabrication to replace petroleum-based polymer. Compared to starches and proteins from edible sources such as maize, tapioca, potato, and soy, the materials from agro-waste are thought to be better sources to avoid controversy of using potential food for use in composite fabrication.

Due to the hydrophilic characteristic of MFC, using it in hydrophobic polymers is not regarded as effective. However, some techniques could address this non-compatibility issue by chemically modifying MFC, including TEMPO-mediated oxidation[85] and esterification[86]. Chemical treatment, however, may damage the intrinsic 3-D network structure of the MFC. The mechanical properties of the chemically treated MFC composites did not exhibit expected mechanical improvement though better dispersity was obtained.[87]

To reinforce hydrophobic polymers by unmodified MFC, some techniques have been put forward.[87–89] MFC/PLA composites were successfully fabricated by papermaking-like fabrication

process and water-based methods by pre-treating PLA in water in the form of microparticles. MFC/PLA composites using both above mentioned techniques exhibited good dispersion and resulted in enhanced mechanical properties.[87–89]

2.3 Liquid crystalline cellulose (LCC) fibers: production, modification and composite fabrication

2.3.1 Production of LCC fibers

Despite the outstanding mechanical properties of pure cellulose materials, plant based fibers have relatively inferior mechanical properties. For example, their tensile strength is much lower than 1,000 MPa, with most common fibers ranging between 200 MPa and 500 MPa, compared to glass fibers that have strength of 2,000 to 3,000 MPa.[90] Alignment of microfibrils at an angle to the fiber axis, defects, variations in plant growing conditions and inherent impurities such as lignin, hemicellulose, etc., affect the strength of these fibers.[91] As a result, most green composites based on natural cellulosic fibers have tensile strengths and Young's moduli in the range of about 100 to 200 MPa and 4 to 8 GPa, respectively.[12,13,53,60,92] These properties of green composites, while sufficient for non-critical applications such as food packaging, furniture and decoration, etc., are not sufficient for load-bearing structural applications such as construction, automotive or aerospace. One other major difficulty with plant based fibers is that they are not continuous, i.e. short length and, hence, must be spun or twisted to form continuous yarns. This further reduces their effective strength and Young's modulus and limits their applications.

There are already several methods to make uniform and continuous cellulose multifilament yarns including rayon® and Lyocell®, by changing their chemistry or dissolving cellulose in some specific solvents and using traditional wet or dry spinning techniques, to obtain the cellulose fibers

with uniform and much smaller diameter and in continuous form.[93] Although the processes have been established for producing continuous cellulose fibers, the tenacity and modulus of these fibers are even lower than the plant based fibers.

The latest development of dissolving cellulose in certain solvents to form liquid crystalline cellulose solution has been significant. Liquid crystalline state is the phase between solid and liquid. Materials have mobility like liquid but with molecules organized in 3-D crystalline structure, retain their anisotropic charateristic.[94,95] When liquid crystalline cellulose solution is formed in a solvent and spun using the air gap-wet spinning system, the high molecular orientation that already exists in the liquid crystalline state is retained. For example, Kevlar®, Zylon® are produced from liquid crystalline solutions which maintain high orientation and results in very high strength and modulus.

One method to produce liquid crystalline cellulose is to use phosphoric acid. Phosphoric acid has been proven to be good solvent for cellulose for a long time but its anisotropic behavior was discovered quite late.[95] Boerstoel showed that superphosphoric acid which is obtained by adding phosphoric acid to the melt of orthophosphoric acid, can dissolve cellulose fast to form a viscous and birefringent solution.[94] Liquid crystalline cellulose solution could then be formed in polyphosphoric acid solvent which avoids damaging the anisotropic behavior of cellulose solution.[95] After filtering, spinning, stretching and washing, liquid crystalline cellulose (LCC) fibers were obtained with high strength in the range of 1.5-1.7 GPa with fracture strain of 6.5% and Young's modulus of 44 GPa. These have been the highest tensile properties obtained for any continuous cellulose fibers.

2.3.2 Modification of LCC fibers and fabrication of advanced green composites

Because of the excellent tensile properties, continuous nature and inherent biodegradability, LCC fibers have been regarded as promising reinforcing fibers to make 'advanced green composites' with much higher strength and stiffness.[96–98] When biodegradable resins are combined with LCC fibers, fully biodegradable composites can be fabricated. LCC fibers have been used to make advanced green composites to reinforce soy protein based resins.[96,97] Researchers have found that the hydroxyl groups on LCC fibers provided good hydrogen bonding with the polar groups such as amine, carboxyl and hydroxyl groups present in SPC, increasing the fiber/resin interfacial interaction and resulting in good composite properties.[96,97] LCC fibers have been also combined with starch to make advanced green composites with excellent properties.[98]

Although LCC fibers have high strength and modulus, they can be treated by chemical, mechanical and thermal means to further enhance the molecular orientation and crystallinity and increase their strength and Young's modulus. One modification method has been alkali treatment similar to the mercerization process commonly used for cotton fibers to improve their properties.[90,97] Kim and Netravali found that LCC fibers, when treated under tension (load) during alkali treatment, significantly improved the orientation of cellulose molecules as well as their crystallinity.[97] This resulted in enhancement in LCC fiber strength from 1.5 GPa to over 1.7 GPa and Young's modulus from 48 GPa to over 64 GPa.[97] When 40 wt% of these treated LCC fibers were used with soy protein isolate (SPI) based resin, composites with high strength of 652 MPa and Young's modulus of 24 GPa were obtained.[97] In another study by Rahman and Netravali, LCC fibers were treated with 5% $NaHSO_3$ solution along with tension.[98] These fibers then underwent further thermal drying treatment. The strength of the treated fibers increased over 35%, close to 2 GPa.[98] When composites were formed by combining the modified LCC fibers (M-LCC) with a

waxy maize starch/MFC, the strength of the composites increased by over 50% from 505 MPa for raw LCC fiber composites to 790 MPa for M-LCC fiber composites.[98] It was thought that the strength of the LCC fibers could increase to over 2 GPa if the solvent type, loading weight and time of tension, temperature and time of the thermal treatment could be optimized.

CHAPTER 3: EXPERIMENTAL METHODS

3.1 Materials

Raw avocado seed powder (*Persea Americana v. Hass*) was obtained from a local supplier in Ithaca, NY. Velvet leaf plants were collected from a local farm in Ithaca, NY. Microfibrillated cellulose (MFC) (Celish KY-100G) was purchased from Daicel (Japan), Inc. Liquid crystalline cellulose was obtained from Dr. H. Boerstoel, Teijin Twaron BV, Arnheim, and sodium hydroxide (NaOH) and potassium hydroxide (KOH) pellets were purchased from Sigma-Aldrich (St. Louis, MO). 1,2,3,4-butane tetracarboxylic acid (BTCA) and sodium hypophosphite monohydrate (SHP) were obtained from Alfa Aesar (Haverhill, MA). Sorbitol, glycerol and sodium chlorite were purchased from VWR (Radnor, PA). Glacial acetic acid, was obtained from EMD Millipore Corporation (Burlington, MA).

3.2 Starch purification from avocado seed powder

Raw avocado seed powder was first dried in an air-circulating oven at 45 ℃ for two days. Dried seed powder was then sieved through a 250 μm (60-mesh) screen. In the next step 200 g of sieved avocado seed powder was mixed with 2L deionized (DI) water and stirred at 700 rpm at room

temperature (RT) overnight. The obtained suspension was processed in a kitchen blender (Oster®) for 5 min before passing through three layers of cheesecloth.[24] The solid part that contained mostly ash, residue of seed coat and other undissolved parts remained on the cheesecloth, while most of the starch passed through the cheesecloth. The filtrate was allowed to settle for 3 h until the starch granules precipitated. The supernatant, which contained dissolved soluble sugars, soluble protein, etc., was decanted.[20,22] The precipitated part, which contained most of the starch, was collected.[20,22] The precipitated starch was further washed in DI water three times and poured onto a Teflon® sheet mold to dry in an air circulating oven at 40 ℃ for 48 h. The dried avocado starch was ground in a kitchen blender for 10 min and then passed through a 250 μm (60-mesh) screen again to obtain purified avocado seed starch (AVS) powder. The purified AVS powder was analyzed for its composition by Dairy One, company based in Ithaca, NY. Starch, soluble sugar, protein, ash and moisture content of AVS powder were determined.

3.3 Preparation of crosslinked (thermoset) avocado seed starch (AVS) sheets

Solution casting method was used to obtain the crosslinked pure starch resin sheets to characterize their properties. Five grams of AVS were dispersed in 100 ml of DI water, stirred at 300 rpm and heated to 90 ℃ for 45 min until the starch was completely gelatinized. During gelatinization the viscosity of the suspension greatly increased showing characteristic gel-like behavior.[25] At this time 15% (by wt. of AVS) of sorbitol was added to the gelatinized AVS as the plasticizer. To crosslink the starch, BTCA (20% by wt. of AVS) as crosslinker and sodium hypophosphite (SHP) as catalyst (50% by wt. of BTCA) were added separately and stirred for 1 h at 300 rpm.[25] Gelatinization of starch exposes the hydroxyl groups and, thus, increases the rate of

crosslinking reaction with carboxyl groups in BTCA to form ester links.[25] After cooling, the pre-cured starch slurry was poured onto Teflon® plates (10 cm × 10 cm) and dried in an air-circulating oven for 48 h at 45 ℃ to obtain sheets. After drying, the starch resin sheets were peeled off from Teflon® plates and pressed, individually, in a hot press (Carver, 3891-4PROA00, Wabash, IN) at 140 ℃ for 15 min to complete any additional crosslinking. The hot pressed flat resin sheets were found to be suitable for characterizing their properties. Hot pressing was carried out under a small pressure of 1.4 MPa. The crosslinked sheets were conditioned at ASTM conditions of 65% relative humidity (RH) and 21 ℃ for three days prior to further characterization.

3.4 Purification with velvet leaf microfiber stem fibers (VLF)

Stems of the velvet leaf weed were used as the microfiber source. By repetitive alkali and bleaching treatment, cellulose can be purified and single microfibers released from bundles.[66] Fifty grams of velvet leaf stem were collected from the field in Ithaca, NY, their outer skins and inner spongy cores were removed and only the woody part was retained. The woody part was ground with DI water in a Ninja ultima blender (model BL 800) at 24,000 rpm setting for 10 min. The solid pulp was then collected using a cheesecloth and dried in an air-circulating oven for 2 days before the chemical treatment step.

The dried velvet leaf stem pulp obtained in the mat form was treated chemically to remove lignin and hemicellulose using a 2-step process.[66] The 1st step involved bleaching of pulp using acidified sodium chlorite solution (1 wt% sodium chlorite, 5 wt% acetic acid) and heating at 75 ℃ for 1 h. In this step most of the lignin was removed. The solid was filtered and washed until wash water pH was 7. The second step involved removing hemicellulose using an alkali treatment process in

which the lignin-free solid fiber mass was further treated in 2 wt% NaOH at 80 ℃ for 2 h. The fiber mass was washed with water until pH of 7. Bleaching and alkali treatments were repeated twice until the fibers turned white. The fibers were kept in the form of water-based slurry to prevent fiber drying and aggregation. Cellulose fiber content in the VLF slurry was determined by calculating the weight of the slurry and the solid fiber weight after freeze-drying.

3.5 Preparation of green composites

MFC has been shown to serve as a strong reinforcing agent in green composites.[99] Because of the high aspect ratio the fibrils in MFC can also bridge microcracks and increase the toughness. To combine MFC with AVS based resin, predetermined amounts of MFC slurry (Celish KY-100G, 10%) was dispersed into DI water (1:10) and homogenized at a speed of 20,000 rpm for 10 min using VWR 250 homogenizer (Radnor, PA). The weight proportions of MFC:AVS were predetermined as 10:90, 20:80, 30:70 and 40:60. The MFC dispersions were stirred at high speed at 1,000 rpm overnight to prevent aggregation. This step was followed by slowly adding the pre-weighed AVS powder into the fiber dispersion and mixing for 1 h. The starch-fiber mixture was then heated at 90 ℃ for 45 min followed by adding sorbitol (or glycerol, 15% of total weight of starch and fiber, or no plasticizers), BTCA (20% of starch weight) as the crosslinker and SHP (50% of BTCA weight) as the catalyst. The entire mixture was allowed to react for 1 h before casting on to Teflon® plates (10 cm × 10 cm) to obtain sheets. The sheets were dried for 2 days in an oven at 45 ℃ and hot-pressed at 140 ℃ and 1.4 MPa pressure for 15 min to control the thickness to about 0.5 mm as well as to complete the crosslinking reaction. For fabricating green composites reinforced with VLF, identical process was used with the exception that the homogenization was

not used for VLF microfiber dispersion to avoid microfiber breakage during homogenization. The green composites were conditioned at ASTM conditions of 65% relative humidity (RH) and 21 ℃ for three days prior to further characterization.

Table 1. Specimen nomenclature of starch-based resin sheets and composites

Code	Reinforce Source	Cellulose: starch proportion	Plasticizer (by wt. of both cellulose and starch)	Crosslinker (by wt. of starch)
CSN-0	None	0	15% sorbitol	20% BTCA
CSM-1/9	MFC	10:90	15% sorbitol	20% BTCA
CSM-2/8	MFC	20:80	15% sorbitol	20% BTCA
CSM-3/7	MFC	30:70	15% sorbitol	20% BTCA
CSM-4/6	MFC	40:60	15% sorbitol	20% BTCA
CSV-1/9	VLF	10:90	15% sorbitol	20% BTCA
CSV-2/8	VLF	20:80	15% sorbitol	20% BTCA
CSV-3/7	VLF	30:70	15% sorbitol	20% BTCA
CSV-4/6	VLF	40:60	15% sorbitol	20% BTCA
USM-3/7	MFC	30:70	15% sorbitol	0
USV-3/7	VLF	30:70	15% sorbitol	0
CGM-3/7	MFC	30:70	15% glycerol	20% BTCA
CNM-4/6	MFC	40:60	None	20% BTCA
CNV-4/6	VLF	40:60	None	20% BTCA

The component nomenclature used for various specimens in Table 1 are as follows: first letter indicates crosslinked (C) or noncrosslinked (U), second letter indicates the type of the plasticizer used: sorbitol (S), glycerol (G) or none (N), third letter indicates the type of reinforcing fiber used: MFC (M), VLF (V) or no reinforcement (N), the number at the end shows the fiber/AVS

proportion. Plasticizers were added based on the total weight of starch and cellulose. BTCA was added only based on starch weight.

3.6 Alkali and heat treatment of LCC fibers

Raw LCC fibers were treated by chemical, mechanical and thermal methods to further increase the molecular orientation as well as the crystallinity and thus enhance their modulus and fracture strength.[98] LCC yarns were immersed into 1M KOH diluted solution in a small tank, keeping them under tension by fixing one end of the yarns with clamps and applying predetermined tension using standard weights at the other end as shown in Figure 5.[12,97,98] The chemical (KOH) treatment was carried out for 1.5 h under the tension of 0.7 kg/yarn during the treatment. After the chemical immersion under tension, LCC yarns were rinsed in DI water several times until neutral pH was obtained for the wash water. One batch of alkali treated LCC yarns was dried overnight in an oven at 40 ℃ without any tension. Another batch of LCC yarns, after both alkali and heat treatments, was dried at 140 ℃ in an air-circulating oven for 1 h under the same tension of 0.7 kg/yarn.[98] Both raw (untreated) LCC fibers, alkali treated LCC fibers and modified LCC fibers (with both alkali and heat treatments) were conditioned at 21 ℃ and 65% RH for 24 h before tensile testing. The chemical/tension treated LCC fibers are termed as modified LCC (M-LCC) fibers.

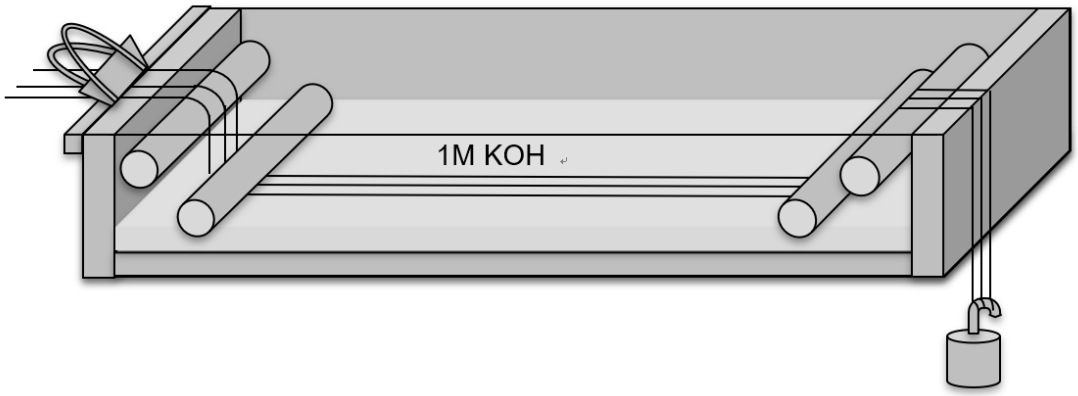

Fig. 5 Schematic illustration of the alkali treatment apparatus

3.7 Preparation of hybrid advanced green composites reinforced by LCC and M-LCC

Because of the brittleness and poor mechanical properties of AVS, 30% MFC (by wt) was added to reinforce the AVS resin. All MFC/AVS resins were then reinforced by aligned LCC or M-LCC fibers to form hybrid advanced green composites. Plasticizer, either sorbitol or glycerol (15% by wt. of MFC + AVS on dry basis), was added to the resin to explore how different plasticizers affect the mechanical properties of the green composites.

Approximately 30 yarns of LCC (or M-LCC) were aligned to form a composite strip of about 25 cm × 2 cm dimensions. The yarns were soaked into MFC/AVS resin and gently squeezed by hand to ensure good resin penetration between the single fibers within the yarn.[98] LCC yarns were then aligned parallel into two layers, unidirectionally, on a Teflon® coated metal mold.[53] Additional resin was poured to cover the fibers/yarns and dried in oven at 40 ℃ for 1 day. After drying, composites were compressed on a Carver Hydraulic hot press (Carver, 3891-4PROA00, Wabash, IN) for 15 min at 140 ℃ and a pressure of 7.5 MPa to further provide compression and

thus improve the interaction between the LCC fibers and the MFC/AVS resin. Six composite strips with the dimensions of 100 mm × 3 mm were cut by laser and conditioned at 21 ℃, 65% RH for three days. The density of LCC (cellulose), MFC (cellulose), AVS (starch) are all roughly about 1.5 g/cm^3. The volume fraction of LCC fibers was determined by the following equation [92]:

$$V_f = \frac{\frac{W_f}{\rho_f}}{\frac{W_f}{\rho_f} + \frac{W - W_f}{\rho_r}}$$

where V_f is the volume fraction of LCC fibers, W_f and W are the weights of LCC yarns and composites, respectively, and ρ_f, and ρ_r are the densities of LCC fibers and resin, respectively.

The component nomenclature of LCC (M-LCC) reinforced MFC/AVS composites with different plasticizers and their LCC fiber volume fractions are presented in Table 2.

Table 2. Specimen nomenclature of LCC fiber reinforced MFC/AVS composites

Composite Code	Resin	Plasticizers	Aligned LCC fiber Volume
LCC-N-MFC/AVS	30:70 MFC/AVS	None	LCC/41.1%
LCC-S-MFC/AVS	30:70 MFC/AVS	15% sorbitol	LCC/37.4%
LCC-G-MFC/AVS	30:70 MFC/AVS	15% glycerol	LCC/38.7%
M-LCC-S-MFC/AVS	30:70 MFC/AVS	15% sorbitol	M-LCC/39.0%

3.8 Characterization of extracted avocado seed starch powder (AVS)

3.8.1 Chemical analysis of starch

The purified AVS powder was analyzed for its composition by Dairy One, company based in Ithaca, NY. Starch, soluble sugar, protein, ash and moisture content of AVS powder were determined.

3.8.2 Rheological properties of starch

Reaching gelatinization temperature is critical to rupture the starch granules and expose the hydroxyl groups present on amylose and amylopectin molecules to provide easy access for the crosslinker to react. To characterize the rheological properties and confirm complete gelatinizing of AVS, Rheometer-2000 (TA Instruments, Inc., New Castle, DE) with a steel plate of 60 mm diameter was used. Constant shear rate of 20 s^{-1} was applied in this test and the gap between the two plates was set to 1,000 μm. The temperature was raised from 20 ℃ to 95 ℃ at a ramp rate of 20 ℃/min for this study.

3.8.3 Scanning Electron Microscopy (SEM)

The shapes and sizes of starch granules and their gelatinization behavior at different temperatures (room temperature, 65 ℃, 80 ℃, 95 ℃,) were characterized using LEO 1550 field emission SEM (Germany). Single droplets of starch suspension at room temperature, 65 ℃, 80 ℃, 95 ℃, were taken out from the rheometer and put on aluminum specimen mounts with double sided conductive carbon tape (SPI supplies, West Chester, PA), individually, and dried at room temperature (RT) overnight. The specimens were carbon coated using a Denton vacuum coater (BTT IV, Denton Vacuum, Moorestown, NJ). The SEM was operated at a low accelerating voltage of 1~2 kV to avoid any charging.

3.9 Characterization of velvet leaf microfibers (VLF)

3.9.1 Attenuated total reflectance-Fourier transform infrared (ATR-FTIR) analysis

ATR-FTIR spectroscopy was used to confirm proper purification of VLF. ATR-FTIR spectra were obtained using Thermo Nicolet Magna-IR 560 spectrometer with a split pea accessory. Each scan was an average of 150 scans from 4000 cm^{-1} to 600 cm^{-1} wavenumbers.

3.9.2 Distribution of length, diameter and aspect ratios of microfibers (VLF)

To measure the length, diameter and to calculate aspect ratios (L/D) of VLF microfibers, small amount of microfiber slurry was randomly picked and diluted with DI water until single microfibers could be observed in optical microscopy (Olympus BX51, Hamburg, Germany). Three hundred and twenty (320) microfibers from optical microscope images were randomly picked and their lengths and diameters were measured using Image J analysis software. At least five separate spots were picked on each single microfiber to calculate the average diameter. SEM was also used to characterize the VLF fiber shapes and size by using LEO 1550 field emission SEM (Germany). Diluted VLF fiber suspension were put on aluminum specimen mounts with double sided conductive carbon tape (SPI supplies, West Chester, PA) and dried overnight. The SEM procedure used was identical to that described in section 3.8.3.

3.10 Characterization of crosslinked starch

3.10.1 Attenuated total reflectance-Fourier transform infrared (ATR-FTIR) analysis

ATR-FTIR analysis was used to estimate the ester formation of crosslinking reaction. The process used was same as described in section 3.9.1

3.10.2 Differential scanning calorimetry (DSC)

DSC Q2000 (TA Instruments, Inc., New Castle, DE) was used to characterize thermal properties of the crosslinked starch films. Between 0.5 mg and 2 mg of every specimen (film) were weighed and put, individually, in hermetically sealed aluminum pans. The temperature was raised from 30 ℃ to 350 ℃ at a ramp rate of 10 ℃/min to obtain the DSC thermograms.

3.11 Characterization of green composites

3.11.1 Thermogravimetric analysis (TGA)

Degradation temperatures of various specimens were obtained using thermogravimetric analyzer TGA-2050 (TA Instruments, Inc., New Castle, DE). About 10 mg of raw AVS powder, crosslinked AVS sheets or cellulose reinforced AVS composites were scanned from 30 ℃ to 600 ℃ at a ramp rate of 10 ℃/min to obtain the TGA thermograms.

3.11.2 Swelling power and moisture absorption analysis

Swelling behavior of the specimens (10 mm × 20 mm) was characterized to determine the water stability of the sheet according to the ASTM standard D570-98. To accomplish this MFC/AVS green composite specimens were first dried in an air circulating oven at 50 ℃ for 24 h and weighed. Specimens (sheet) were then immersed in a beaker containing DI water for 3 days. After every 24 h, the specimens were taken out, wiped with Kimwipes® to remove the surface water and weighed using a microbalance with a resolution of 0.0001 g.

The percent increase in weight, i.e., water absorption, was calculated from the equation below.

$$\text{Water absorption (\%)} = \frac{M - M_0}{M_0} \times 100\%$$

where M_0 is the weight of the dried specimen before water absorption and M is the weight of the specimen after being immersed in DI water for 1, 2, 3 days.

To obtain the moisture regain of the sheet specimens, they were conditioned for five days at ASTM conditions of 21 ℃ and 65% RH. Weights of specimens were observed to stabilize at the end of 5 days as they reached equilibrium moisture absorption. After five days, specimens were dried in an oven for 1 day at 50 ℃. The weight of dried specimen was measured again using the same balance. The moisture regain (%) was calculated using the equation below

$$\text{Moisture regain (\%)} = \frac{M_5 - M_0}{M_0} \times 100\%$$

where M_5 is the weight for 5 days of conditioning and M_0 is the weight of the specimen after drying.

3.11.3 Dynamic mechanical analysis (DMA)

Specimens were analyzed for their dynamic mechanical properties using TA DMA Q800 (TA Instruments, Inc., New Castle, DE). The DMA instrument was set to conduct tests in single cantilever mode. The specimens were clamped, individually, at one end and the other ends were flexed. Specimens were cut to specific width of 5.0 mm and length of 30 mm, and tested from -60 ℃ to 100 ℃ at a ramp rate of 5 ℃/min and the applied strain rate and frequency were 0.1% and 1 Hz, respectively. Dynamic mechanical properties such as storage modulus (E'), loss modulus (E"), and tan δ were obtained from these tests.

3.11.4 Tensile properties of crosslinked starch sheets and green composites

The crosslinked starch resin and MFC/AVS, VLF/AVS green composite sheets were cut to dimensions of 10 mm × 50 mm. These specimens were conditioned at 21 ℃ and 65% RH for three days prior to conducting the tests using an Inston 5566 universal tester (Instron Corp., Canton,

MA) according to ASTM D882-02. The mechanical properties including tensile (fracture) stress, tensile (fracture) strain and Young's modulus were obtained from these tests. The thicknesses of the specimens were measured using a digital caliper at five locations within the gauge length and the average values were used for calculations. The gauge length and strain rate of the specimens tested were 30 mm and 0.6 min^{-1}, respectively. At least five specimens were tested for each condition. Average values of fracture stress, fracture strain and their standard derivation were obtained from the raw data obtained from Instron tests. Young's modulus values were calculated using OriginLab software.

3.11.5 Fracture surface topographies analysis of green composites

The fracture surfaces of MFC/AVS and VLF/AVS composites were characterized using LEO 1550 field emission SEM (Germany). For observing composite fracture surfaces, composite specimens were mounted on aluminum specimen mounts using a double-sided conductive carbon tape and then coated with carbon using a Denton vacuum coater (BTT IV, Denton Vacuum, Moorestown, NJ). The SEM procedure used was identical to the description in section 3.8.3.

3.12 Characterization of treated LCC (M-LCC) fibers

3.12.1 Fiber surface characterization

The surfaces of single LCC fibers before and after alkali treatment were observed in SEM. Same procedure of SEM was used as described in section 3.8.3.

3.12.2 Tensile properties of LCC and M-LCC fibers

LCC and M-LCC fibers were tensile tested as per ASTM D3822-01 using Instron 5566 universal tester (Instron Corp., Canton, MA). Single LCC fibers were glued using Super Glue®

(cyanoacrylate) to individual paper tabs to obtain 50 mm length gauge length as shown in Figure 6. The fiber diameters were determined by optical microscopy (Olympus BX51, Hamburg, Germany). Diameters of fibers were measured at five different locations within the gauge length and the average diameter was used for calculating tensile properties. Fibers were conditioned at 21 ℃ and 65% RH for 24 h before tensile testing. At least 10 specimens were tested to obtain average properties. To carry out the test, two ends of the paper tab were mounted in the Instron grips and the two sides of the paper tab were cut around the dash line in Figure 6 on both sides so as to have full load on the fiber. All tests were carried out at a strain rate of 0.1 min^{-1}.

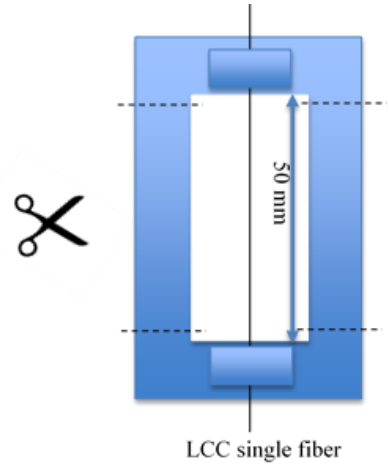

Fig. 6 Schematic illustration of the paper tab used for LCC fiber tensile tests

3.13 Characterization of LCC reinforced hybrid advanced green composites

3.13.1 Tensile analysis of advanced green composites

The tensile testing of LCC/M-LCC reinforced MFC/AVS green composites was carried out as per ASTM D3039-17. Composite specimens were laser cut to dimensions of 3 mm × 100 mm and

conditioned at 21 ℃ and 65% RH for three days prior to testing. Gauge length and strain rate were set to 50 mm and 0.1 min^{-1}, respectively.[98] The average thickness of each composite specimen was measured and found to be 0.65 mm. The average fracture stress and strain values were calculated from the raw data obtained from Instron. Young's modulus values were calculated using OriginLab software. At least 5 specimens were tested to get average values. Also, specimens fabricated at three different times were tested to confirm the reproducibility.

3.13.2 Fracture surface topographies of advanced green composites

The fracture surfaces of tensile tested LCC/M-LCC reinforced MFC/AVS green composites were characterized using a LEO 1550 field emission SEM (Germany). The SEM procedure used was identical to the description in section 3.8.3.

CHAPTER 4: RESULTS AND DISCUSSION

4.1 Characterization of extracted avocado seed starch (AVS)

4.1.1 Chemical analysis of AVS

Table 3. Chemical components of raw avocado seed powder and purified seed starch (AVS)

Constituents	Raw seed powder (%)	AVS (%)
Moisture	8.9	4.3
Dry Matter	91.2	95.7
Starch	53.5	80.7
Starch (Dry wt. basis)	58.7	84.3
WSC (Water Sol. Carbs.)	4.7	2.6
ESC (Simple Sugars)	1.8	0.7
Crude Protein	4.0	2.7
Adjusted Crude Protein	4.0	2.7
Crude Fiber	3.5	2.0
Crude Fat	2.9	0.6

As mentioned earlier, purified AVS powder was obtained by removing the impurities including protein, sugars and ash using simple water filtration technique. Table 3 presents the components of avocado raw seed powder before and after purification (AVS). Results show that after purification overall starch content significantly increased from 53.5 to 80.7% and on dry weight basis (without the moisture) the increase was from 58.7% to 84.3%, while the crude and adjusted crude protein, fibers, fat, sugars and ash all decreased to below 3%. The purity of AVS was sufficiently high for crosslinking and using it as resin fabricating green composites.

4.1.2 Rheological properties of AVS

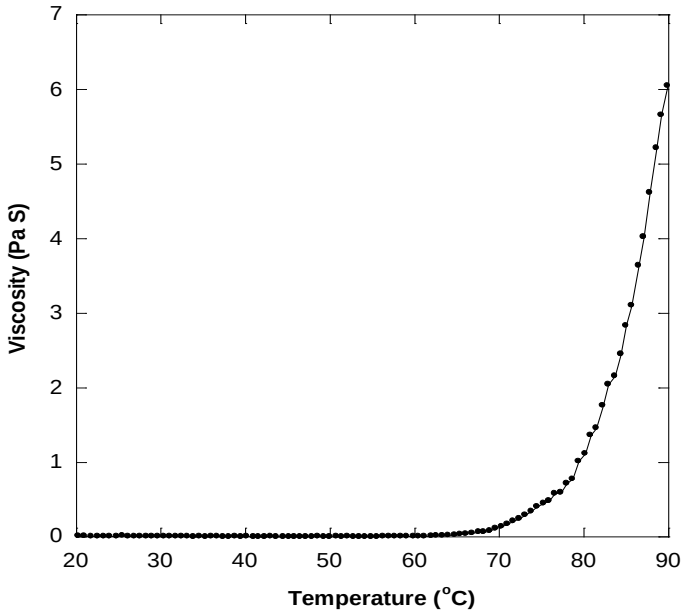

Fig. 7 Plot of viscosity vs temperature of AVS solution

Starch granules are insoluble in water at room temperature. However, when temperature is raised, starch granules allow water to penetrate the cell wall and start swelling. The granules continue to swell as they absorb more water and finally rupture. Once inside, water acts as a plasticizer and breaks the crystalline structure of starch.[52] Figure 7 shows the change in viscosity of avocado starch suspension as the temperature is increased from 20 ℃ to 90 ℃. It can be observed that the viscosity does not change when the starch is in the form of granules. However, once the temperature goes above 80 ℃ the granules start rupturing and allow starch molecules to come out. As a result, the viscosity rises rapidly.

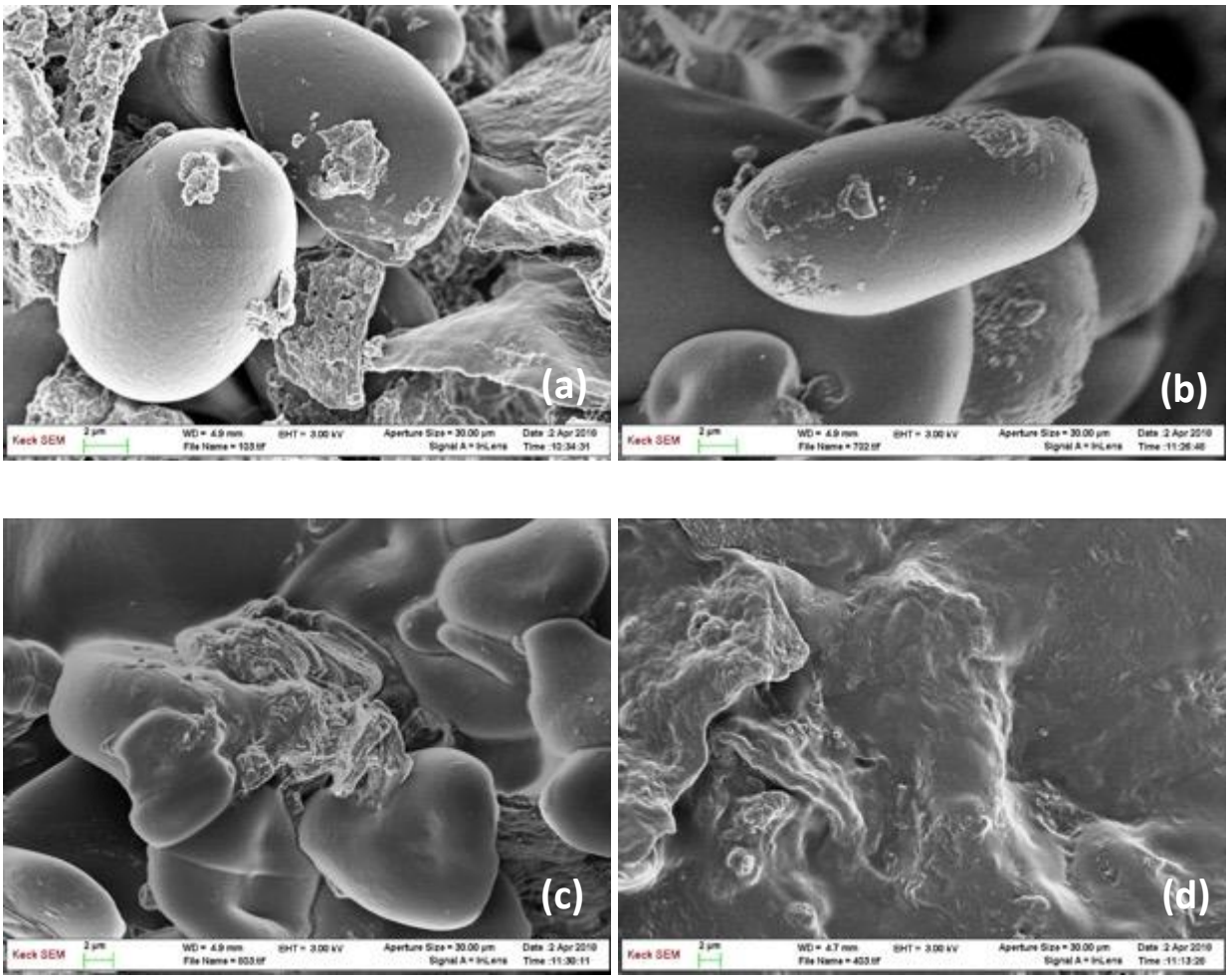

Fig. 8 SEM images of AVS starch granules taken at four temperatures (a) room temperature, (b) 65 ℃, (c) 80 ℃ and (d) 95 ℃

SEM images of AVS starch granules taken at four temperatures are shown in Figure 8. From these images the size of avocado seed starch granules was found to be in the range of 5 to 20 µm. As stated earlier, when temperature reaches 80 ℃, the starch granules start to rupture and at temperatures of over 90 ℃, most granules rupture and a homogeneous gelatinized solution is formed. Once gelatinized, at this high temperature, starch sheet can be formed by solution casting. From viscosity measurements and SEM observations, it was concluded that 80 ℃ is closer to the gelatinizing temperature of AVS. Since starch molecules are no more confined within the granules

above the gelatinizing temperature, the hydroxyl groups are fully exposed and, as a result, provide much higher possibility for chemical crosslinking reaction to take place.[52]

4.2 Characterization of velvet leaf microfibers (VLF)

4.2.1 Attenuated total reflectance-Fourier transform infrared (ATR-FTIR) analysis

As described earlier VLF was obtained by a combination of alkali and bleaching treatments that removed both hemicellulose and lignin without affecting the cellulose. Due to the chemical similarity between cellulose and starch, both consisting of glucose units, microfibers with higher purity of cellulose (content) can be expected to have better fiber/resin adhesion, through hydrogen bonding, making the reinforcement more efficient.[46]

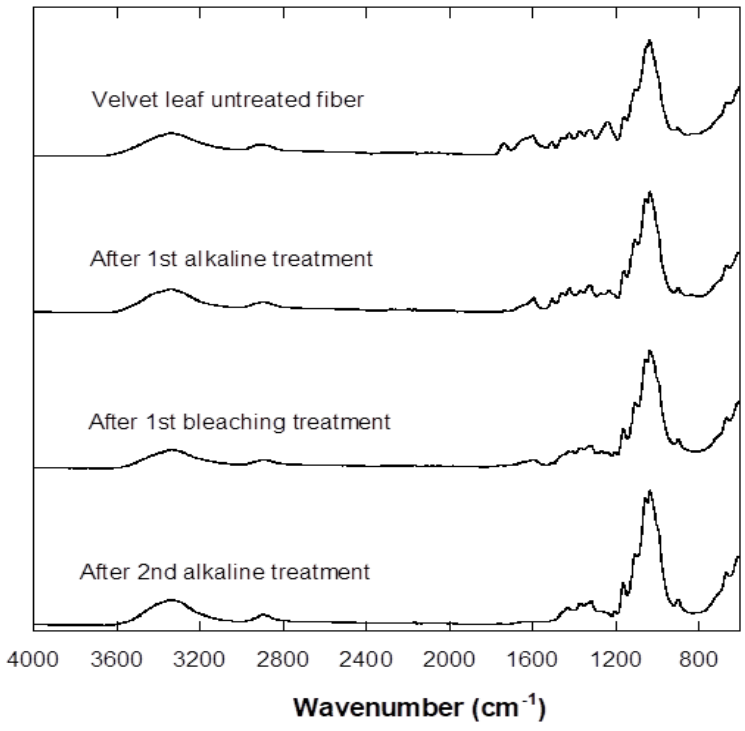

Fig. 9 ATR-FTIR spectra of VLF fibers, untreated and after each treatment

Figure 9 shows ATR-FTIR spectra of untreated (control) and treated VLF fibers. The spectrum for untreated velvet leaf fiber pulp showed a characteristic peak at 1736 cm^{-1} which is unconjugated stretching of carbonyl group from carboxylic or ester groups present in hemicellulose.[53] It also contains C-O-C stretching vibration of aryl alkyl ether groups at 1240 cm^{-1} and phenyl backbone aromatic C=C bending at 1500 cm^{-1} for lignin.[12] After the first alkali treatment, the carbonyl peak at 1736 cm^{-1} disappeared, confirming the removal of hemicellulose. Bleaching using $NaClO_2$ has been a common practice to remove lignin with phenyl structure.[66] The peaks at 1240 cm^{-1} and 1500 cm^{-1} almost disappeared after bleaching. The second alkali treatment served to remove both unwashed ClO^{2-} and the lignin residue that remained after bleaching reaction. The ATR-FTIR spectrum of the final VLF product showed that treated velvet fiber slurry was white with high cellulose purity and suitable for making green composites.

4.2.2 Distribution of length, diameter and aspect ratios of MFC and VLF microfibers

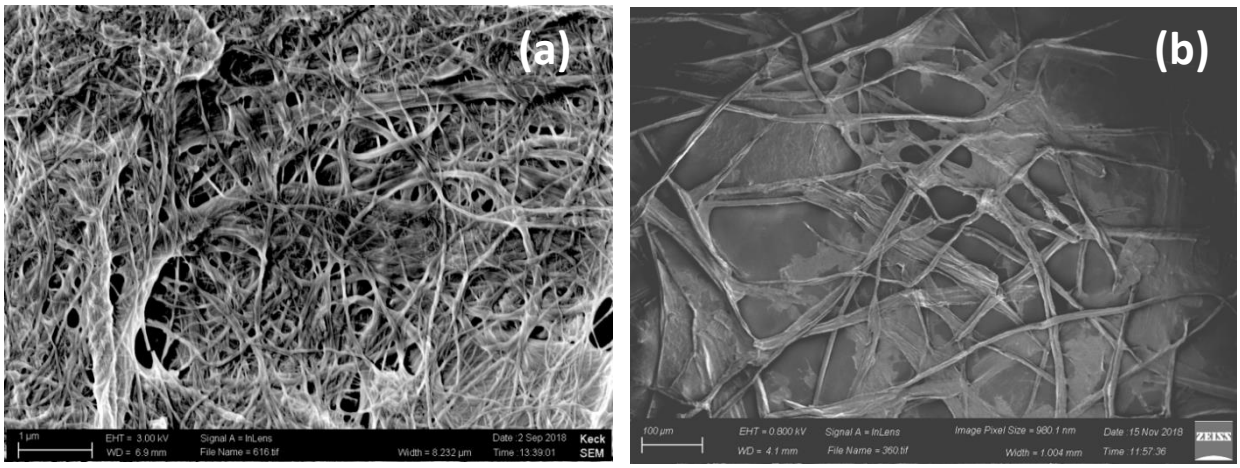

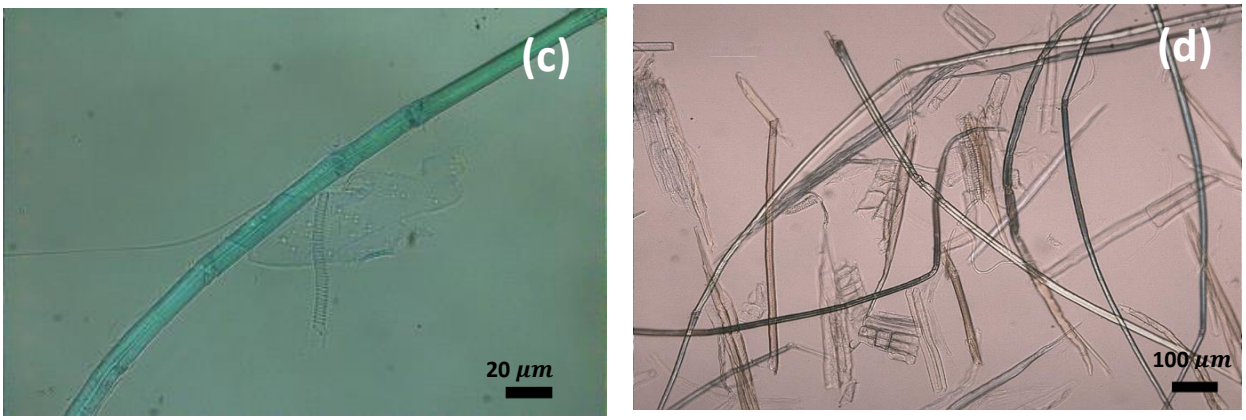

Fig. 10 SEM images of (a) MFC, (b) VLF and optical microscopy images at different magnifications of (c) VLF and (d) VLF

Figures 10 (a) and (b) show SEM images of nanoscale MFC and micro-scale VLF. Diameters of both MFC and VLF could be easily measured from these images. Compared with VLF having individual fibers with average diameter of about 12 μm, MFC shows an entangled 3-D network with single fibril diameters of around 50 nm. The length and aspect ratio of VLF, could only be gauged from optical microscopy images as can be seen in Figures 10 (c) and (d). Aspect ratios of microfibers can greatly impact the mechanical properties of reinforced composites.[62,100] Higher aspect ratio of fiber reinforcement is known to result in higher tensile strength and Young's modulus in composites because they bridge microcracks formed under stress and cannot be easily pulled out from the resin in the fracture zone.[62,100] However, fibers with very high aspect ratios might easily aggregate and/or entangle making it difficult to obtain uniform dispersion in the resin. Since bleaching and alkali treatments remove undesired lignin and hemicellulose from VLF, they also serve to separate the bonded fibers. As a result, after the treatments, single fibers are individualized. Many factors can influence the aspect ratio of the treated VLF microfibers. First, fibers from different parts of the plant as well as those extracted in different seasons would have

different quality as well as aspect ratios of microfibers. Second, different treatment variables such as speed and duration of velvet leaf stem grinding, concentration of bleaching and alkali agents and treatment times, could have significant effect on their lengths and diameters and, hence, on the aspect ratios of VLF microfibers.[46]

The distribution of fiber lengths, diameters and aspect ratios of VLF are presented in Figure 11. Length of most of the microfibers ranged between 200 and 1000 µm and diameters between 10 and 18 µm resulting in aspect ratios between 10 and 50. Values for average length, diameter and aspect ratio were 897 µm, 15.2 µm and 69.0, respectively. However, nearly 10% of the treated VLF had lengths higher than 1.5 mm and aspect ratios greater than 100. It may be assumed that microfibers with longer lengths and higher aspect ratios would dominate the reinforcement effect even though they were relatively small in number.

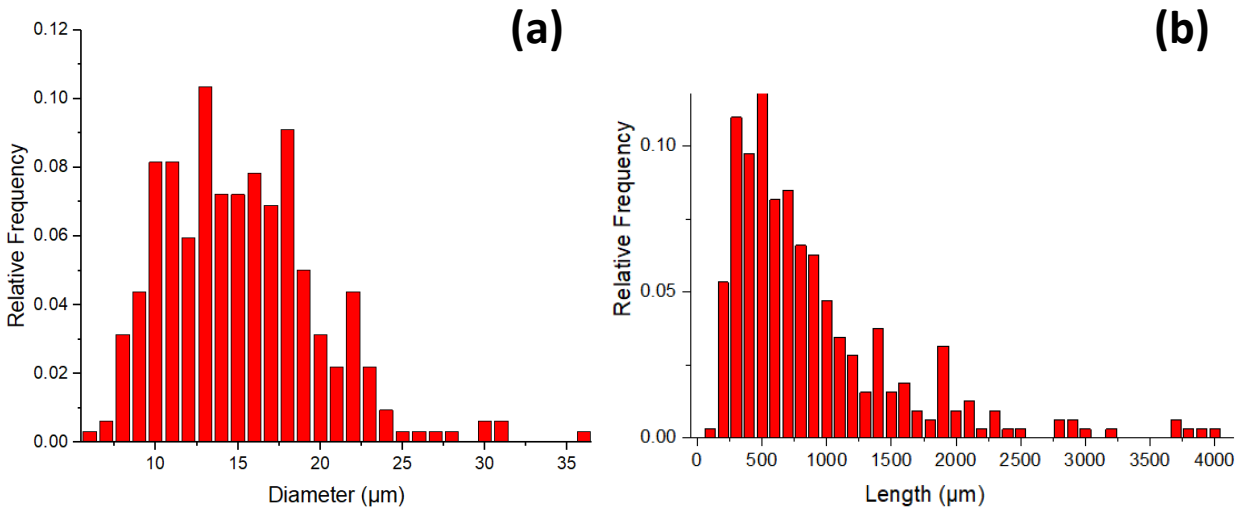

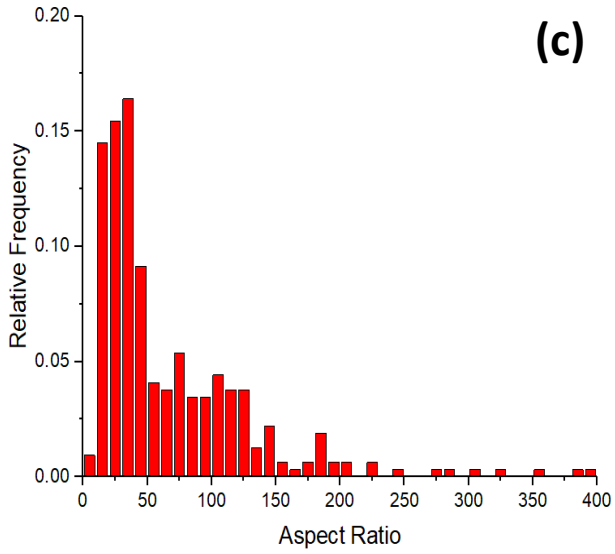

Fig. 11 Distributions of (a) fiber length, (b) diameter and (c) aspect ratios of VLF

4.3 Characterization of crosslinked starch sheets

4.3.1 Attenuated total reflectance-Fourier transform infrared (ATR-FTIR) analysis

Predetermined amounts of BTCA (crosslinker) and SHP (catalyst) were added to the starch suspension at 90 °C to crosslink the starch. At this temperature, BTCA can react, at least partially, with starch molecules that are in the gelatinized state. Solution casting method was then used to obtain the resin sheets. Partially crosslinked or pre-cured sheets were obtained after drying. The pre-cured sheets were further crosslinked by hot-pressing to obtain fully crosslinked resin sheets. Time and temperature of hot pressing process can greatly influence the extent of crosslinking.[35,36] Waxy maize starch and mango seed starch have been successfully crosslinked earlier using BTCA.[24,25] These studies concluded that 15 min at 140 °C were sufficient to obtain comparably high degree of substitution (DS).[24,25]

Higher extent of crosslinking of starch means less hydroxyl groups remain, i.e., less moisture absorption by the resin. However, if excess amount of BTCA is used, both unreacted BTCA and catalyst (SHP) serve as additional plasticizers which absorb water and lower the mechanical properties of the resin. To dissolve and remove any unreacted BTCA trapped inside starch resins, previous studies washed the resin with water and combined it with ultrasonification.[25,34,52] However, water washing also removes other desired plasticizers such as sorbitol or glycerol which can make resins brittle and undesirable for composite fabrication and packaging applications. The amount of crosslinker, thus, should be optimized to minimize water absorption and maximize the mechanical properties. Sorbitol or glycerol (15% by wt. of AVS), which are both highly soluble in water, were used in crosslinked AVS resin sheet fabrication.

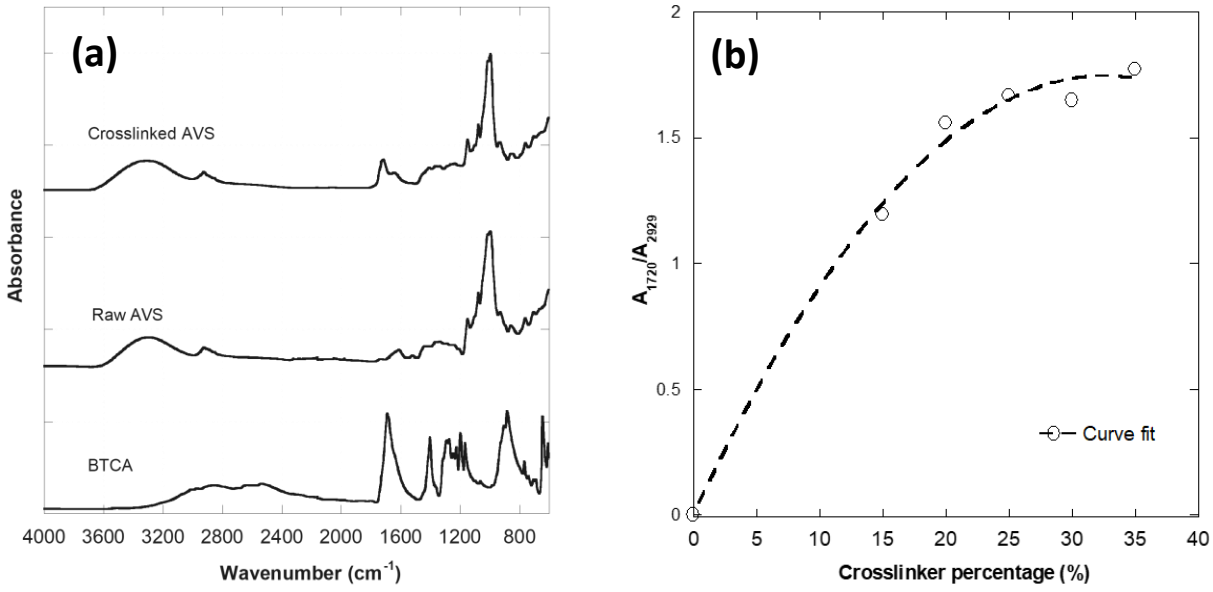

Fig. 12 Determination of crosslinking extent by ATR-FTIR (a) ATR-FTIR plots of crosslinker BTCA, raw AVS and crosslinked AVS resin and (b) the value of A_{1720}/A_{2929} of crosslinked AVS resin vs BTCA concentration from 15% to 35%

ATR-FTIR spectra of crosslinked AVS resin sheets prepared with different concentrations of BTCA were obtained to determine the optimal amount of BTCA. Figure 12 (a) presents the ATR-

FTIR spectra of raw AVS, crosslinked AVS and BTCA. As mentioned in an earlier study, the peak at 1720~1725 cm^{-1} represents carbonyl ester stretching and the peak at 2929 cm^{-1}, which is constant, represents C-H stretching and could be used as a reference peak.[34] Thus the ratio A_{1720}/A_{2929} has been considered to positively correlate with the extent of crosslinking.[34] To confirm the extent of crosslinking, crosslinked AVS sheets prepared with BTCA concentrations of 15%, 20%, 25%, 30% and 35% (by wt. of AVS) were fabricated and washed overnight to remove unreacted BTCA which partially overlaps with ester peak. ATR-FTIR spectra were utilized to measure the relative absorbance of ester peak value and compare their extent of crosslinking. The polynomial curve of A_{1720}/A_{2929} ratio as a function of BTCA percentage is shown in Figure 12 (b). The value of A_{1720}/A_{2929} ratio continues to increase with higher BTCA amount. However, at 20% BTCA, A_{1720}/A_{2929} ratio was close to saturation, showing that BTCA amount just about 20% might be needed to obtain a high extent of crosslinking.

4.3.2 Differential scanning calorimetry (DSC)

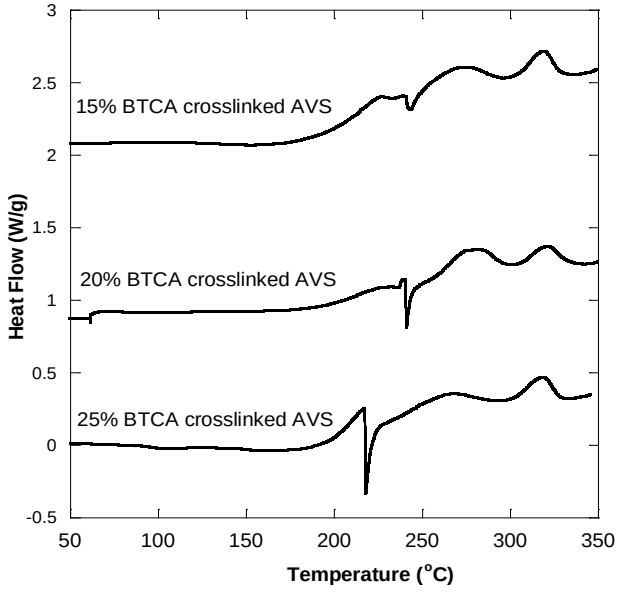

Fig. 13 DSC thermograms of crosslinked starch with BTCA concentrations of 15, 20 and 25%

DSC was used to further confirm the BTCA amount needed to crosslink starch films. Figure 13 shows DSC thermograms of crosslinked AVS resin sheets containing BTCA concentrations of 15, 20 and 25%. Unwashed crosslinked AVS sheets were used to test the amount of unreacted BTCA trapped in sheets. AVS resin with 15, 20 and 25% of BTCA were run on DSC to observe BTCA melting. The BTCA melting enthalpy values were found to be 3.89, 11.12 and 32.5 kJ/g for 15, 20 and 25% BTCA concentrations, respectively, showing that a large part of BTCA remained unreacted in resins prepared with 25% BTCA. The enthalpy for unreacted BTCA drastically reduced when the BTCA proportion was reduced from 25% to 20% and further to 15%. From both ATR-FTIR and DSC results, it was obvious that 20% BTCA would be the optimum concentration to crosslink AVS. As a result, all composites were fabricated using AVS resin crosslinked with 20% BTCA.

4.4 Characterization of green composites containing MFC or VLF

4.4.1 Thermogravimetric analysis (TGA)

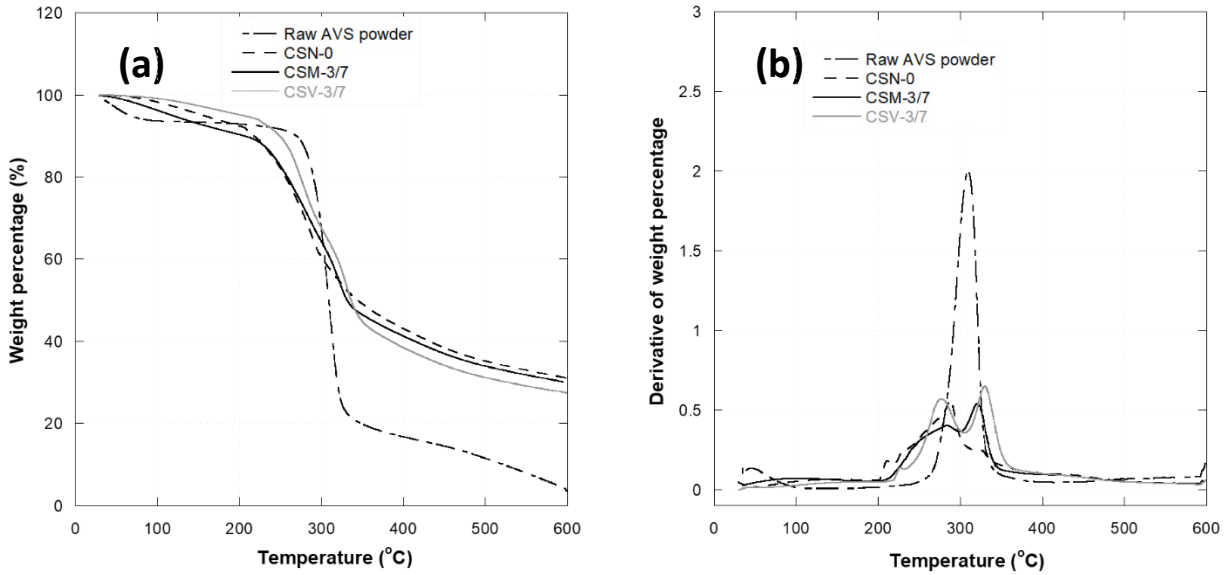

Fig. 14 TGA (a) and DTGA (b) thermograms of raw AVS powder, CSN-0, CSM-3/7 and CSV-3/7 composites

Table 4. Thermal degradation of starch and composite specimens

Specimen	Initial degradation temperature (℃)	Maximum peak I degradation temperature (℃)	Maximum peak II degradation temperature (℃)
Raw AVS powder	280.1	309.9	/
CSN-0	231.4	288.1	/
CSM-3/7	230.7	284.1	325.4
CSV-3/7	228.8	277.6	330.1

Figure 14 shows TGA and DTGA thermograms of raw AVS powder, crosslinked starch sheet CSN-0, and green composites CSM-3/7 and CSV-3/7. TGA thermograms provide a good indication of the thermal stability of raw starch powder, crosslinked starch and crosslinked composites containing MFC (CSM) or VLF (CSV). Onset degradation temperature and maximum degradation temperature obtained from Figure 14 are presented in Table 4. Raw AVS showed an initial degradation temperature of 280 ℃ whereas crosslinked starch and composites showed lower onset degradation temperatures in the range of about 230 ℃. Generally, the degradation temperature should be higher. However, the low degradation temperature in this case can be attributed to the existence of unreacted carboxylic groups of BTCA, i.e., BTCA itself, which degrades at lower temperature.[24] After adding MFC or VLF, the thermal stability did not demonstrate improvement for either CSM-3/7 and CSV-3/7 composites compared with CSN-0. This shows that the degradation temperature of cellulose fiber and AVS do not have any impact on each other as they remain separate.[25,52] Crosslinked AVS and MFC/AVS and VLF/AVS composites, due to the rigid 3-D crosslinked network structure, showed higher amount of char at 600 ℃. For DTGA plots shown in Figure 14 (b), two peaks around 275~285 ℃ and 325~330 ℃ were obtained for both MFC/AVS and VLF/AVS composites. These peaks confirm degradation

of starch and cellulose, respectively. This also proves that both starch and cellulose components degraded without interference of the other part.[10,75] This can be expected because fibers and resin stay as separate phases and have different degradation temperatures.

4.4.2 Swelling power and moisture absorption analysis

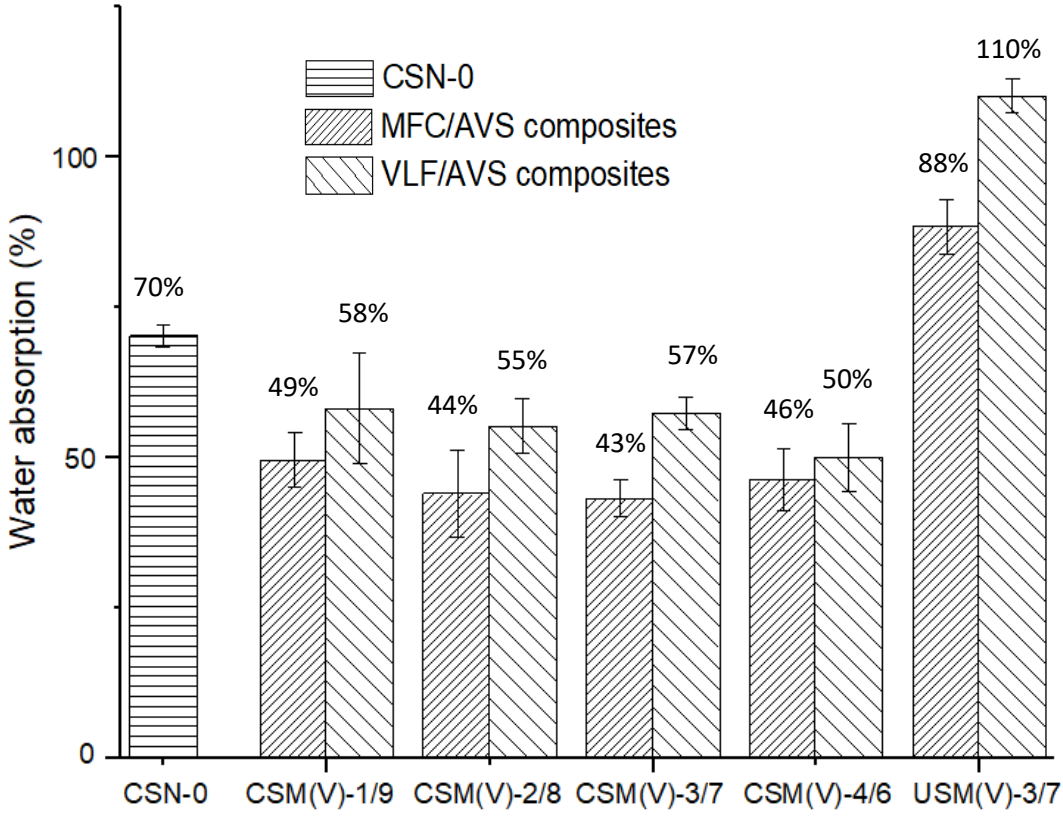

Fig. 15 Water absorption plots for MFC/AVS and VLF/AVS composites and crosslinked starch resins measured after 24 h of water immersion

For all specimens immersed in DI water, water absorption increased during first 24 h and then remained stable. The water absorption (%) at the 3rd day, for crosslinked composites CSM-1/9~CSM-4/6, CSV-1/9~CSV-4/6, noncrosslinked composites USM-3/7, USV-3/7, and crosslinked resin CSN-0, are presented in Figure 15. As can be seen in Figure 15, for noncrosslinked specimens USM-3/7 and USV-3/7, 88 and 110% wt. gains, respectively, were

obtained. After crosslinking, as expected, water absorption decreased significantly to 43 and 57% for CSM-3/7 and CSV-3/7, respectively. Crosslinked AVS resins have rigid structure, less hydroxyl groups and low capacity to expand/swell, thus reduced water absorption can be expected. Similar results were observed in previous studies on crosslinked soy protein isolate (SPI), neem protein as well as waxy maize starch resins.[24,25,34–36,83] Lower water absorption is beneficial in composites as it indicates increased water stability. Also, absorbed water can swell the composites and reduce their Young's modulus and fracture stress significantly.[19]

The effects of cellulose fiber loading can also be seen in the data presented in Figure 15. Cellulose is hydrophilic and readily absorbs water in the amorphous regions. It is believed that 5 to 10 wt% of water could be absorbed by cellulose materials such as MFC and VLF fibers at ASTM conditions of 65% RH and 21 ℃.[101] However, because of the significantly higher crystallinity of individual cellulose nanofibers in MFC and higher fiber/resin hydrogen bonding, water absorption of cellulose reinforced starch composites could be lower.[29,76,102,103] In this study the crosslinked starch sheets without any cellulose reinforcement showed 70% water absorption. The water absorption reduced to around 40% to 50% for MFC and 50% to 60% for VLF containing composites, respectively. For MFC-reinforced AVS composites, significant decrease in water absorption (49%) occurred when MFC was content was 10%. However, when the MFC content increased to 40%, water absorption was 46%, which was statistically insignificant ($p > 0.05$) with 10% MFC content. VLF reinforced AVS composites also showed increasing resistance to water absorption. At 10% VLF content the composites absorbed 58% water and at 40% VLF content composites absorbed about 50%. Relatively higher water absorption occurred in VLF/AVS compared with MFC/AVS. This is believed to be because of highly crystalline nature of MFC as

well as its nanoscale 3-D network structure that prevents water absorption through restricted swelling.

4.4.3 Dynamic mechanical analysis (DMA)

Table 5. DMA data of MFC/AVS and VLF/AVS composites

Sample	Storage Modulus		Tan δ		Loss modulus	
	Onset temperature of E' drop (℃)	E' value at 20℃ (MPa)	Temperature at max (℃)	The value at maximum	Temperature at max (℃)	The value at maximum (MPa)
CSM-3/7	-29.1	4810	46.1	0.166	-5.0	1072
USM-3/7	-42.1	3489	-7.6 88.3	0.105 0.193	-20.6	873
CSV-3/7	-31.6	4708	42.3	0.151	-6.6	1049

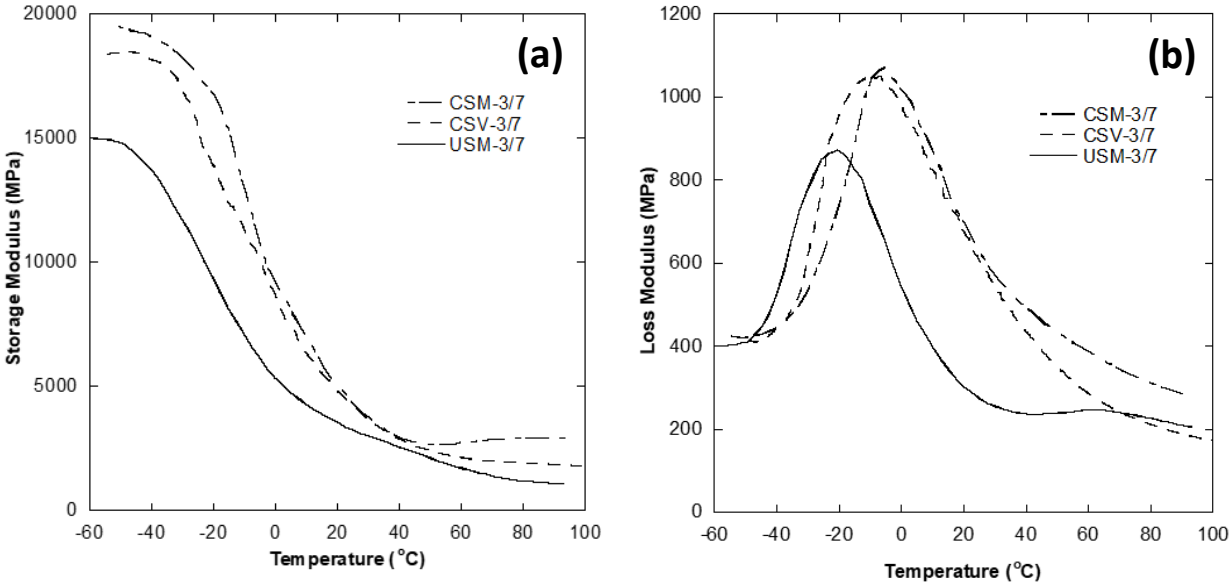

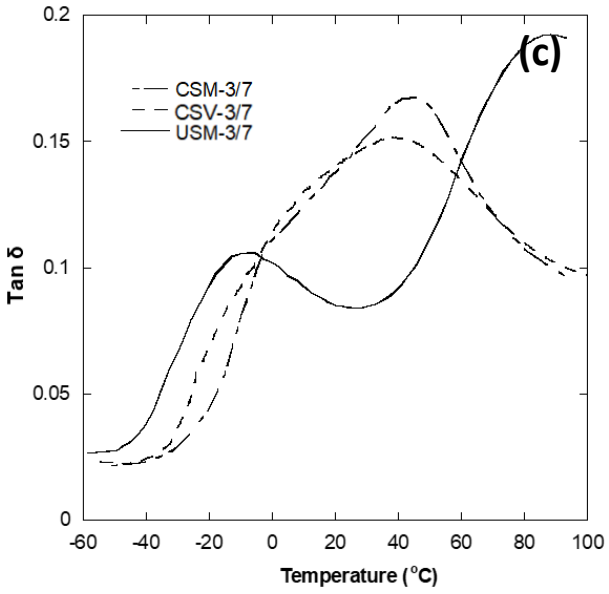

Fig. 16 Storage modulus (a), loss modulus (b) and tan δ (c) of AVS based green composites as a function of temperature

DMA testing was performed to characterize the viscoelastic properties of the AVS based green composites. Table 5 presents the DMA data for composites containing 30% fiber content. The influence of 30% MFC or VLF loading on AVS composites, with or without BTCA crosslinking, on storage modulus, E', loss modulus, E", and tan δ are plotted in Figure 16. In the case of E', the initial drop temperature demonstrates the onset point of chain movement. It can be observed from Figure 16 (a) that when no crosslinker (BTCA) was added (USM-3/7), onset temperature of E' drop was much lower, -42.1 ℃ for USM-3/7 compared to -29.1 ℃ and -31.6 ℃ for CSM-3/7 and CSV-3/7. This suggests that crosslinked 3-D structure is indeed more rigid, as can be expected, and molecular movement starts at a higher temperature than noncrosslinked composites.[104,105] Also, CSV-3/7 composites have comparable onset temperatures and storage moduli at 20 ℃ (4810 MPa of CSM-3/7 and 4708 MPa of CSV-3/7, respectively) to CSM-3/7. This exhibits good reinforcement by VLF which is comparable to MFC. Since VLF is derived from a freely available weed, it can be significantly inexpensive compared to MFC.

Loss modulus, E", plots reflect reinforcement and rigidity of MFC and VLF-based composites.[105] As can be seen from Figure 16 (b), maximum E" peaks for both CSM-3/7 and CSV-3/7 shifted to higher temperatures of -5.0 ℃ and -6.6 ℃ from -20.6 ℃ for USM-3/7. Higher values of 1072 MPa and 1049 MPa were also observed for CSM-3/7 and CSV-3/7, respectively, compared to 873 MPa obtained for noncrosslinked USM-3/7. The higher maximum peak value of crosslinked composites is attributed to the molecular chain hindered by the 3-D network structure, which increases the friction between fiber and starch matrix and, thus, the energy dissipation.[105]

Tan δ is another parameter that measures molecular motion, specifically, the glass transition temperature. One of the important differences between crosslinked and noncrosslinked composites is that only one phase (peak) was observed in tan δ plot for crosslinked composites. Based on earlier studies of cellulose reinforced TPS, the peak at -10 ℃ to 0 ℃ can be attributed to relaxation of the plasticizer (sorbitol)-rich phase and the peak from 40 ℃ to 80 ℃ is the transition within the starch-rich phase.[10,29,37,51,75,76,104,106] This suggests that plasticizer may only partially mix and disperse in starch/cellulose. It is possible that some plasticizer may reside at the fiber/resin interface. Similar results of the separation of two phases are also seen in noncrosslinked specimens USM-3/7 in Figure 16 (c). However, both crosslinked composites CSM-3/7 and CSV-3/7 showed only one tan δ transition peak. It is possible that the hydroxyl groups in sorbitol took part in chemical crosslinking reaction preventing phase separation of starch-rich and sorbitol-rich phases. This suggests that crosslinkers in the resin might help plasticizers disperse better to avoid phase separation. Crosslinking brings molecules closer and hence the resin can show apparent shrinkage when crosslinked. This can provide some pressure at the fiber/resin interface, which can make it difficult for the plasticizer to stay at the fiber/resin interface.

4.4.4 Tensile properties of crosslinked starch sheets and green composites

Table 6. Tensile test data of MFC/AVS and VLF/AVS composites*

Specimen Code	Fracture Strength (MPa)	Fracture strain (%)	Young' Modulus (MPa)	Moisture content (%)
CSM-1/9	13.96 (2.12)**	7.66 (3.82)	1054 (270)	7.54 (0.99)
CSM-2/8	16.00 (1.36)	8.36 (1.95)	1434 (129)	7.72 (0.63)
CSM-3/7	27.23 (1.40)	7.74 (1.96)	1810 (201)	6.67 (0.50)
CSM-4/6	30.56 (2.28)	9.13 (2.01)	2025 (251)	7.18 (0.34)
CSV-1/9	11.90 (1.39)	8.39 (1.41)	787 (148)	7.75 (0.88)
CSV-2/8	21.24 (7.97)	7.30 (2.49)	1444 (617)	7.07 (0.61)
CSV-3/7	27.80 (1.50)	10.18 (1.73)	1614 (204)	6.85 (0.51)
CSV-4/6	40.71 (4.17)	6.44 (0.60)	2744 (550)	6.88 (0.77)
CGM-3/7	18.23 (2.60)	18.69 (4.15)	388 (95)	/
CNM-4/6	46.03 (4.09)	3.56 (0.66)	3896 (533)	/
CNV-4/6	47.10 (3.83)	2.78 (0.45)	4489 (646)	/
CSN-0	3.65 (1.33)	10.95 (6.75)	289 (301)	/
USM-3/7	18.57 (1.99)	8.39 (3.46)	1500 (260)	/

*All specimens were conditioned for 3 days at 21 ℃ and 65% RH
**The numbers in parentheses are standard deviations

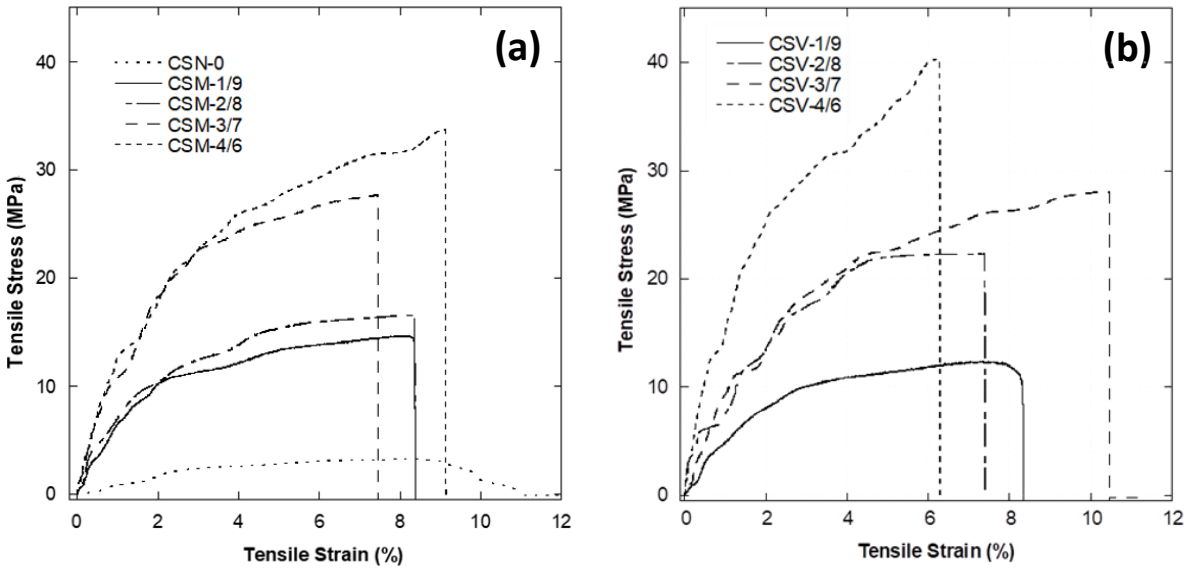

Fig. 17 Typical stress vs strain plots of (a) MFC/AVS and (b) VLF/AVS composites

Results of the tensile tests for MFC/AVS or VLF/AVS composites, with different fiber/resin proportions of 0:10 to 4:6, are presented Table 6. Figure 17 presents typical stress vs strain plots for the same composites. Data for other specimens, containing 15% glycerol (CGM-3/7), without sorbitol (CNM-4/6 and CNV-4/6), without fiber reinforcing (pure AVS resin with 15% sorbitol) (CSN-0) and without crosslinker BTCA (USM-3/7) are also listed in Table 5 for comparison.

For specimens CNM-4/6 and CNV-4/6, without any plasticizers, high fracture stress (> 45 MPa) and high Young's modulus (> 4 GPa) were obtained, as was expected. However, their brittle nature with relatively low fracture strain (less than 3.5%) might prevent these materials from being applied in packaging and other fields. Glycerol was also used in CGM-3/7. High fracture strain can be attributed to better diffusion and plasticization of glycerol compared with sorbitol.[29,38] The fracture stress and Young's modulus, however, reduced drastically because of the breakage of intermolecular hydrogen bonding by glycerol. As stated earlier, to avoid significant loss of fracture stress, for all other composites sorbitol (15%) was used as the plasticizer. Sorbitol did lower the

fracture stress from 45 MPa for CNM-4/6 to around 30 MPa for CSM-4/6. However, this level of plasticization by sorbitol provides sufficient fracture strain to increase the flexibility, and usefulness in some applications, of AVS-based plastics.

Comparing the results obtained for CSN-0 with CSM-1/9 to CSM-4/6 in Table 6 and stress vs strain plots in Figure 17 (a), the fracture stress and Young's modulus increased from 3.65 MPa for specimens with no MFC (CSN-0) to 30.56 MPa for specimens with 40% MFC (CSM-4/6). The fracture strain, however, remained steady at 8~9% compared to 11% for CSN-0. Researchers have reported severe reduction of tensile strain when just 5~10% of cellulose was added to TPS.[10,76] However, unlike TPS with high fracture strains, crosslinked AVS starch resin with 15% sorbitol had fracture strain of only around 11% while pure MFC sheets usually have fracture strain of 6~8%.[107] The results obtained here clearly indicate that MFC loading of up to 40% does not affect the fracture strain of MFC/AVS crosslinked composites if MFC is uniformly dispersed. However, MFC increases the fracture stress of composites significantly. The high crystallinity and excellent strength of cellulose fibrils in MFC, the high aspect ratio and high surface area and chemical similarity with starch, makes MFC an excellent reinforcing agent for starch based resins.[25,52,106]

Same amounts of VLF were also introduced into AVS starch resin to form composites and the results were compared with MFC/AVS composites. The tensile results for CSV-1/9 to CSV-4/6 specimens are presented in Table 6 and typical stress vs strain plots are shown in Figure 17 (b). It can be seen that when the VLF content was less than 30%, VLF/AVS composites showed mechanical properties comparable to MFC/AVS. Identical fracture stress values were obtained for CSV-3/7 and CSM-3/7 of around 28 MPa but CSV-3/7 demonstrated significantly higher fracture strain (10.2%) compared to CSM-3/7 (7.7%) ($p < 0.05$). Cellulose fibers at nanoscale such as MFC, provide rigid structure than microscale fibers to starch resin due to the higher area of

cellulose/starch interface. While the 3-D network structure of MFC provided higher Young's modulus, fracture strain was lowered. On the contrary, even when there was less VLF/AVS interface area in VLF/AVS composites, high aspect ratio of VLF of about 70 provided strong VLF/AVS interaction and load carrying ability. At significantly lower cost, VLF should be an excellent candidate for reinforcing starch. However, when VLF content was increased to 40%, fiber aggregation was noticed which means that at higher loading fiber dispersity was an issue. Though high fracture stress of 40.71 MPa and Young's modulus of 2744 MPa were obtained for CSV-4/6, the fracture strain reduced to 6.44%. This suggests that 30% of VLF content would be the ideal for VLF/AVS composites.

Water acts as a plasticizer when absorbed by these green composites. The moisture content of all MFC/AVS and VLF/AVS composites were calculated after conditioning them for 3 days at 65% RH and 21 ℃. These results are presented in Table 6. As MFC and VLF content increased from 10% to 30%, the moisture content decreased significantly from about 7.6% to 6.7% ($p < 0.05$). Also, for both MFC/AVS and VLF/AVS composites, 30% fiber content showed the lowest moisture absorption. These results clearly indicate that cellulose fibers do provide better water resistance at 65% RH.

4.4.5 Fracture surface topographies of green composites

To obtain better fiber/resin interfacial bonding, in addition to their chemistries being compatible, it is critical to have uniform dispersion of fibers in the resin. In the present study, since both starch and cellulose are made of glucose units, excellent fiber/resin hydrogen bonding can be expected.[108] Higher fiber/resin interfacial bonding results in better stress transfer from broken fibers to intact fibers.[5] For any composites, fiber breakage at the fracture surface signifies good fiber/resin interaction whereas long protruding fibers signify poor bonding. Figure 18 shows typical SEM

images of crosslinked and noncrosslinked 30% MFC reinforced AVS composite fracture surfaces. Figure 18 (a) shows fracture surface for CSM-3/7 composite fabricated using crosslinked AVS (BTCA, 20%) and Figure 18 (b) shows fracture surface of USM-3/7 composite fabricated with noncrosslinked AVS.

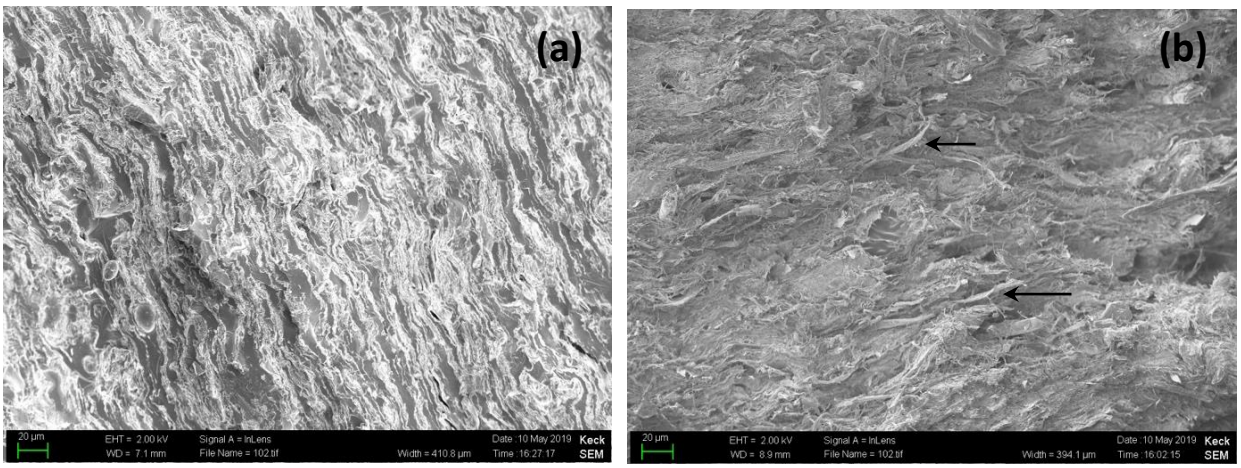

Fig. 18 SEM images of fracture surfaces of MFC/AVS composites: crosslinked (a) CSM-3/7 and noncrosslinked (b) USM-3/7

SEM image in Figure 18 (a) for CSM-3/7 shows almost no protruding fibers whereas SEM image in Figure 18 (b) for USM-3/7 clearly shows several microfibers and even fiber bundles (shown by arrows) protruding at the fracture surface. This suggests that crosslinked AVS starch has better bonding ability with MFC. As mentioned earlier, crosslinks bring molecules closer. This allows the fibers to be squeezed which provides better hydrogen bonding and increases the interfacial shear strength. Another factor could be the possible reaction of BTCA with both starch and cellulose as mentioned by other researchers.[25] This provides covalent bonding which is much stronger than hydrogen bonding and results in significantly better cellulose/AVS interaction.[52] This fracture surface topography confirms the important role of crosslinking with BTCA for improving fiber/resin interfacial bonding.

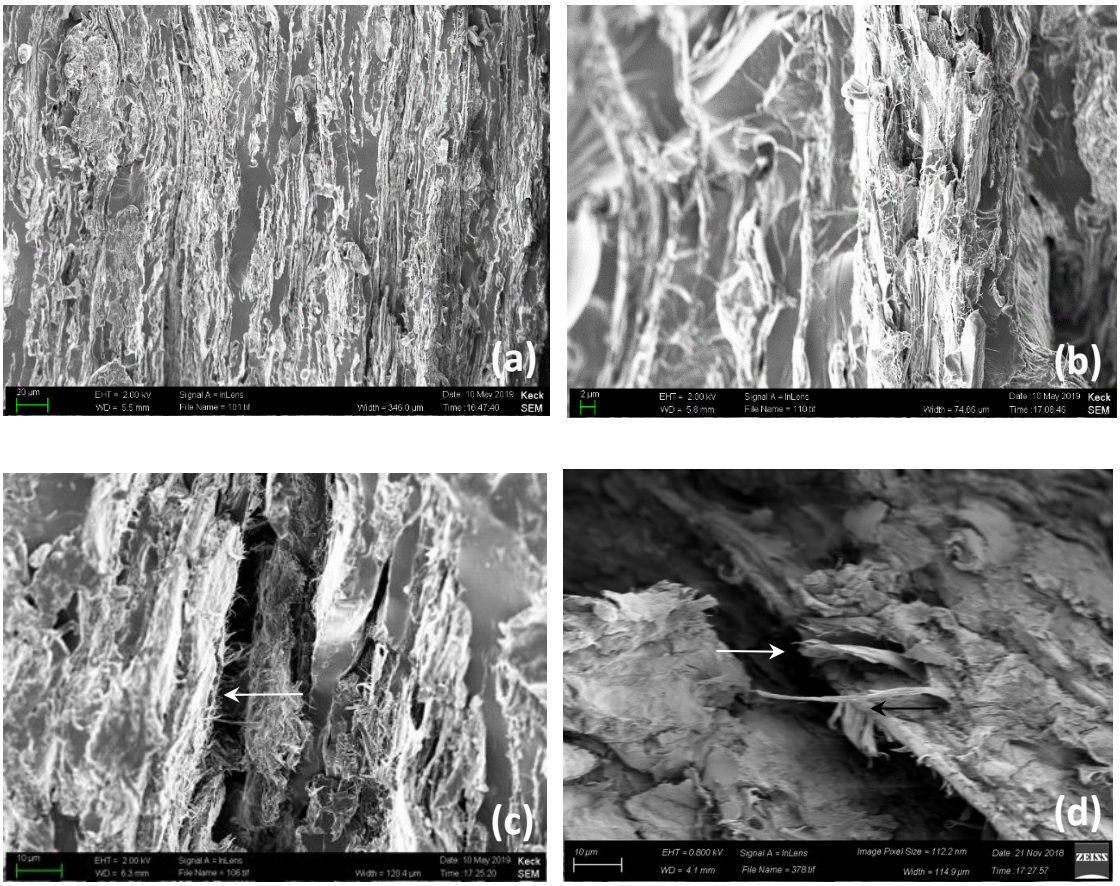

Fig. 19 SEM images of fracture surfaces of crosslinked VLF/AVS green composites (CSV-3/7). (a)~(d) are images for CSV-3/7 composites at different magnifications and different locations.

Typical images of fracture surface topographies of VLF/AVS green composites, taken at different magnifications, are shown in Figure 19. As seen from the SEM image in Figure 19 (a) overall dispersion of VLF seems uniform. However, fiber aggregation, bundles and cracks could still be found at some locations as seen in Figures 19 (b) and (c). The high surface roughness of VLF fibers provides high mechanical bonding and results in strong interfacial interaction. Fiber breakages at the fracture surface, with little protrusion, seen in SEM image shown in Figure 19 (d) confirm good VLF/starch adhesion. This could also be the effect of high aspect ratio making it difficult to pull fibers out. Interfacial bonding between the resin and micro-scale fibers is usually lower compared to nano-scale cellulose because (1) microfibers tend to aggregate or not disperse

uniformly in the resin, (2) have relatively lower fiber/resin interfacial area and (3) cellulose microfibers may not be pure enough and any presence of lignin and hemicellulose can hinder their interaction with starch.[76] Present research confirmed that VLF microfibers, when purified, can provide strong bonding with starch matrix. VLF nanofibrils seen in SEM images presented in Figures 19 (b) and (c), may have been created during bleaching/NaOH treatments or during mechanical mixing with AVS. However, they greatly increase the interfacial bonding with starch and further improve the mechanical properties of the composites.

4.5 Characterization of treated LCC fibers

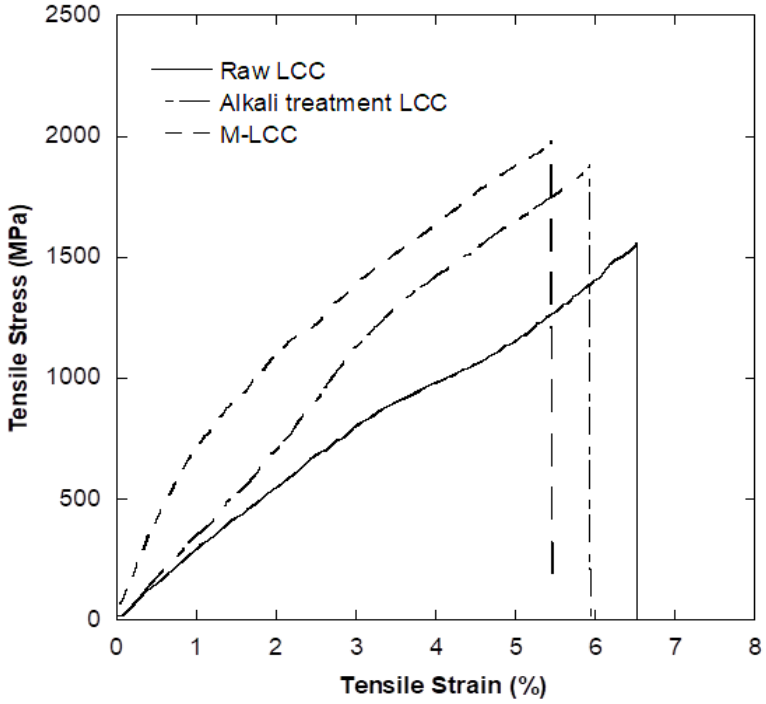

Fig. 20 Typical tensile stress vs strain plots of raw LCC, alkali treated LCC, alkali and heat treated (under stress) LCC (M-LCC) fibers.

Table 7. Tensile test data of raw LCC, alkali treated LCC and M-LCC fibers

Specimens	Fracture stress (MPa)	Fracture strain (%)	Young's modulus (GPa)
Raw LCC	1496 (193)	6.4 (0.2)	49.4 (4.6)
Alkali treated LCC	1854 (161)	6.0 (0.5)	43.2 (6.0)
M-LCC	1908 (178)	5.6 (0.3)	63.9 (3.7)

As-received (control) LCC fibers were produced by an air gap-wet spinning method from a liquid crystalline solution, perhaps without elaborate post-spinning treatments. Previous research clearly showed that LCC fiber properties could be significantly improved with chemical, mechanical and heat treatments that result in increased molecular orientation and crystallinity of the fibers.[97,98] Both KOH and $NaHSO_3$ solutions were used successfully as the chemicals for LCC fiber treatment.

In order to optimize the treatment parameters to further enhance the strength of LCC fibers, the alkali treatment developed by Kim and Netravali was modified by using a weight of 0.7 kg for the LCC yarns and increasing the treatment time to 1.5 h with other factors unchanged.[97] The number of filaments in each LCC yarn were 1,000. The stress loading for LCC fibers was calculated to be 65 MPa/filament, which is 5% of the ultimate fracture stress. The tensile stress vs strain plots of control LCC fibers, alkali treated LCC fibers without heat treatment and alkali treated fibers with heat (M-LCC) are shown in Figure 20 and tensile data are presented in Table 7.

As can be seen from stress vs strain plots in Figure 20 and tensile data in Table 7, alkali and heat treatments resulted in significant enhancement of both the fracture stress and Young's

modulus of LCC fibers. Fracture stress (strength), fracture strain and Young's modulus for untreated (control) LCC fibers were 1496 MPa, 6.4% and 49.4 GPa, respectively. These values are close to those obtained for control LCC fibers in previous studies.[94,97] When the alkali treatment is carried out under tension, microfibrils in LCC fibers get stretched and cellulose molecules get oriented.[97] The rearrangement and extension at both nano- and molecular level leads to significant increases in orientation and crystallinity of LCC fibers and results in the improvement of both fracture stress and Young's modulus.[97,98] For alkali-treated LCC fibers without post-thermal treatment, fracture stress reached 1854 MPa while Young's modulus decreased slightly to 43.2 GPa. The reduction in Young's modulus is perhaps due to some fiber shrinkage or relaxation during slack drying. However, the rearranged morphology after the alkali treatment resulted in 24% improvement of fracture stress to 1854 MPa. It has been observed that during alkali treatment, the molecular structure changes irreversibly and permanently which results in significant improvement in LCC fibers properties.[97] To avoid possible fiber shrinkage and improve Young's modulus, heat treatment with a load the same as that used in the alkali treatment was found to be critical.[98] After both alkali treatment and post-thermal treatment under application of load, less shrinkage occurs. In this study these conditions led to both higher fracture stress of over 1900 MPa and Young's modulus of 64 GPa compared to 1854 MPa and 43.2 GPa, respectively, without the application of heat during drying. At the same time, the tensile strain for M-LCC fibers decreased to 5.6% from 6.0% obtained for control fibers. Based on these results, it was assumed that a 0.7 kg load (65 MPa, 5% of ultimate fracture strength of LCC) was ideal stress level that improves the molecular orientation without causing any morphological damage to LCC fibers.

4.6 Characterization of LCC fiber reinforced hybrid advanced green composites

The effect of plasticizers on the MFC/AVS resin properties has been discussed earlier and presented in Table 6 in section 4.4.4. From the results mentioned in the last paragraph, the average fracture strain of LCC and M-LCC fibers were 6.4% and 5.6%, respectively. In general, to ensure that composites reach their maximum fracture stress, it is important for the resin fracture strain to be greater than that of the fiber.[17] As mentioned earlier, MFC was added to AVS resin to enhance its fracture stress and fracture strain. As discussed earlier, both starch and cellulose are made up of glucose as the monomer and contain hydroxyl (-OH) groups, which allow the formation of hydrogen bonds between the two constituents.[109] In addition, AVS starch was crosslinked using BTCA to enhance its mechanical properties further and improve the water resistance.[24,25] Previous study demonstrated that 30:70 MFC/AVS with 20% BTCA resulted in excellent resin properties without MFC aggregation.[52] As a result, in this study the same 30:70 MFC/AVS combination was used to fabricate advanced green composites with LCC and M-LCC fibers. The effects of plasticizers, 15% sorbitol, 15% glycerol (by wt. of resin), or no plasticizer addition on resin properties were characterized. The tensile test results of MFC/AVS resins with and without the plasticizers are presented in Table 8 and typical stress vs strain plots are presented in Figure 21.

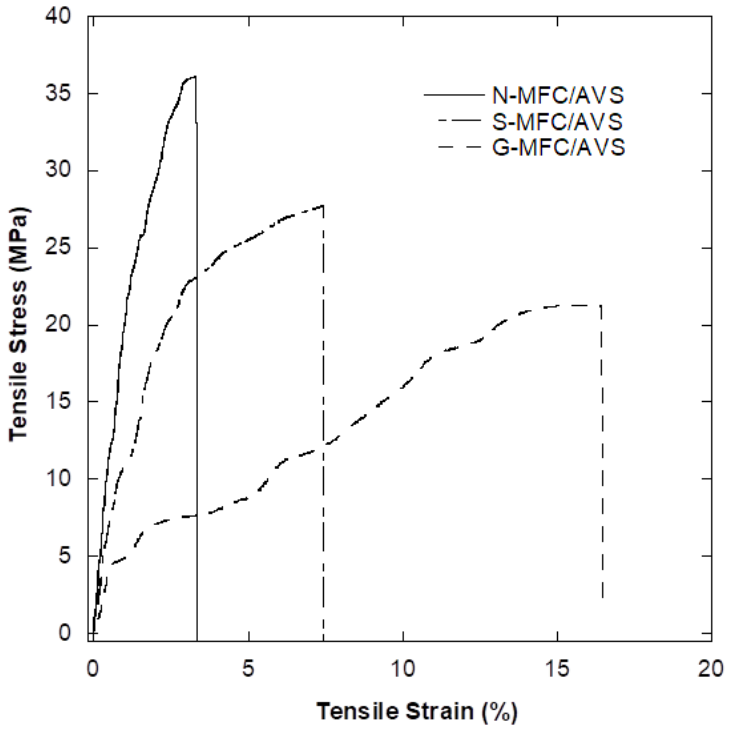

Fig. 21 Typical tensile stress vs strain plots of N-MFC/AVS, S-MFC/AVS and G-MFC/AVS resins

Table 8. Tensile test data of N-MFC/AVS, S-MFC/AVS and G-MFC/AVS resins*

Specimen	Fracture stress (MPa)	Fracture strain (%)	Young's modulus (MPa)
N-MFC/AVS	36.4 (4.1)	3.1 (0.7)	2171 (157)
S-MFC/AVS	27.2 (1.4)	7.7 (2.0)	1810 (201)
G-MFC/AVS	18.2 (2.6)	18.7 (4.2)	388 (95)

*All resins contain 30% MFC and 15% sorbitol or glycerol

The stress vs strain plots in Figure 21 and the data presented in Table 8 for sorbitol or glycerol containing MFC/AVS resins clearly demonstrate the mechanical effects of plasticizers on their mechanical properties. The control MFC/AVS resin without any plasticizer (N-MFC/AVS)

showed brittle characteristics with the fracture strain of just over 3%. This is even lower than the fracture strain of LCC (6.4%) or M-LCC (5.6%) fibers. With the addition of 15% sorbitol or 15% glycerol, fracture strain values of around 7.7% and 18.7%, respectively, were obtained. This means that S-MFC/AVS (with sorbitol) and G-MFC/AVS (with glycerol) resins would be suitable for LCC fiber reinforced green composites. Glycerol is comparatively a smaller molecule than sorbitol. As a result, it is easier to diffuse, penetrate and disperse in the starch-based resin as well as to form a plasticizer layer at the LCC fiber/starch interface.[92] The large amount of free volume added by the plasticizer also results in a much higher fracture strain and a lower fracture stress for the resin.[68,110]

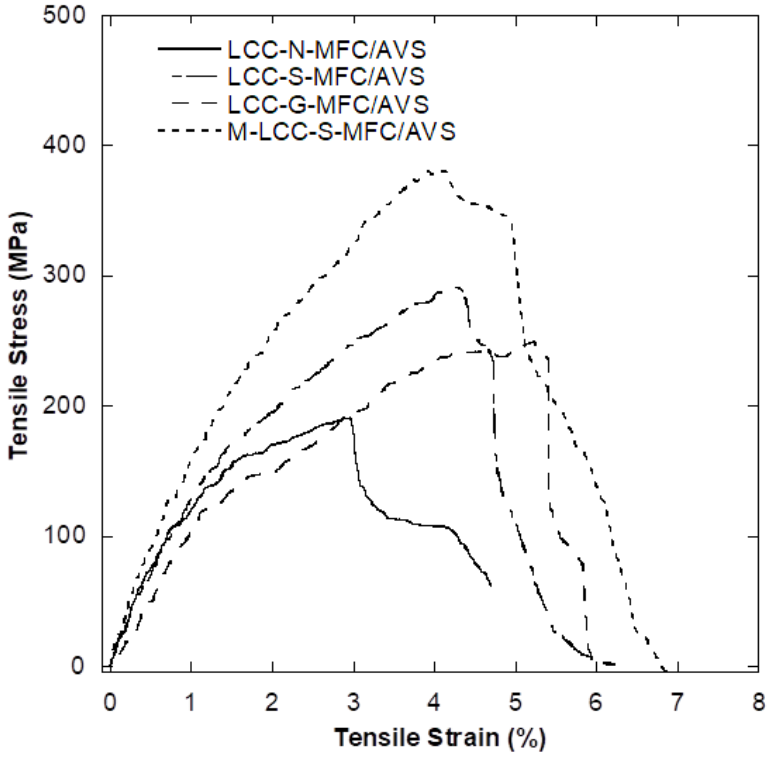

Fig. 22 Typical tensile stress vs strain plots of LCC-N-MFC/AVS, LCC-S-MFC/AVS, LCC-G-MFC/AVS and M-LCC-S-MFC/AVS advanced green composites

Table 9. Tensile test data of LCC-N-MFC/AVS, LCC-S-MFC/AVS, LCC-G-MFC/AVS and M-LCC-S-MFC/AVS advanced green composites

	Fracture stress (MPa)	Fracture strain (%)	Young's modulus (GPa)	Volume fraction of fiber
LCC-N-MFC/AVS	190.1 (24.3)	3.0 (0.4)	16.7 (1.4)	0.411
LCC-S-MFC/AVS	289.8 (35.9)	4.3 (0.7)	15.3 (1.6)	0.374
LCC-G-MFC/AVS	250.8 (26.6)	5.2 (0.8)	12.6 (1.8)	0.387
M-LCC-S-MFC/AVS	380.1 (46.0)	4.1 (0.5)	19.5 (2.4)	0.390

To understand the effect of plasticizers on the properties of LCC fiber reinforced green composites, unidirectional LCC-MFC/AVS composites with 15% sorbitol (LCC-S-MFC/AVS), 15% glycerol (LCC-G-MFC/AVS) and no plasticizer (LCC-N-MFC/AVS) composites were fabricated. LCC fiber volume fraction for all composites was controlled to approximately 40%. The specimens having 3 mm × 100 mm dimensions were tested for their tensile properties, in the longitudinal direction according to ASTM D3039-17. The typical tensile stress vs strain plots are presented in Figure 22 and the data are shown in Table 9.

As can be seen in Figure 22, adding plasticizer (15% sorbitol or 15% glycerol) significantly improved the fracture stress of these composites in comparison to composites that contained no plasticizer. LCC-N-MFC/AVS composites showed a very low fracture strain of only 3.0% and comparably low fracture stress of just over 190 MPa. During the tensile tests brittle resin was always seen to fracture before breaking of the LCC fibers in these composites. This means that the resin N-MFC/AVS could not provide enough strain for LCC fibers to reach their maximum fracture stress. Once the resin failed, there was no mechanism to transfer the stress from broken fibers to intact fibers and other fibers started to fail. After adding plasticizers, the fracture strain of

LCC-S-MFC/AVS and LCC-G-MFC/AVS composites greatly improved to 4.3% and 5.2%, respectively. Data in Table 9 for the resins, discussed earlier, showed that the fracture strains of S-MFC/AVS and G-MFC/AVS resins were much higher than the fracture strain of LCC fibers. This allows LCC fibers to reach their maximum possible stress. However, both LCC-S-MFC/AVS and LCC-G-MFC/AVS composites still had slightly lower strain than the LCC fibers. This could be explained by the defects created during fabrication of the composites or fiber/resin debonding before the fracture of individual LCC fibers.[111] Nevertheless, greatly enhanced fracture stress values of 289.8 MPa and 250.8 MPa were obtained for LCC-S-MFC/AVS and LCC-G-MFC/AVS composites, respectively, after adding sorbitol or glycerol. These values are significantly higher than 190.1 MPa obtained for the LCC-N-MFC/AVS composites, though lower Young's moduli of 15.3 GPa and 12.6 GPa were obtained for LCC-S-MFC/AVS and LCC-G-MFC/AVS composites compared with 16.7 GPa of LCC-N-MFC/AVS. The lower fracture stress, Young's modulus and higher fracture strain of LCC-G-MFC/AVS compared to that of LCC-S-MFC/AVS can be explained by the size and penetration ability of plasticizers which is similar to the plasticization effect of the MFC/AVS resin as discussed before. The smaller molecular size of glycerol can easily penetrate into the resin as well as at both the MFC/AVS and LCC fiber/AVS interfaces.[92] The plasticizer at the fiber/resin interface acts as a lubricant and reduces the interfacial shear strength and, in turn, weakens the composite. The weakened interface leads to both lower fracture stress and Young's modulus while causing a higher fracture strain[68,110] Schematic illustrations presented in Figure 23 show how plasticizers can affect the MFC/AVS resin and the LCC fiber/AVS resin interfaces.

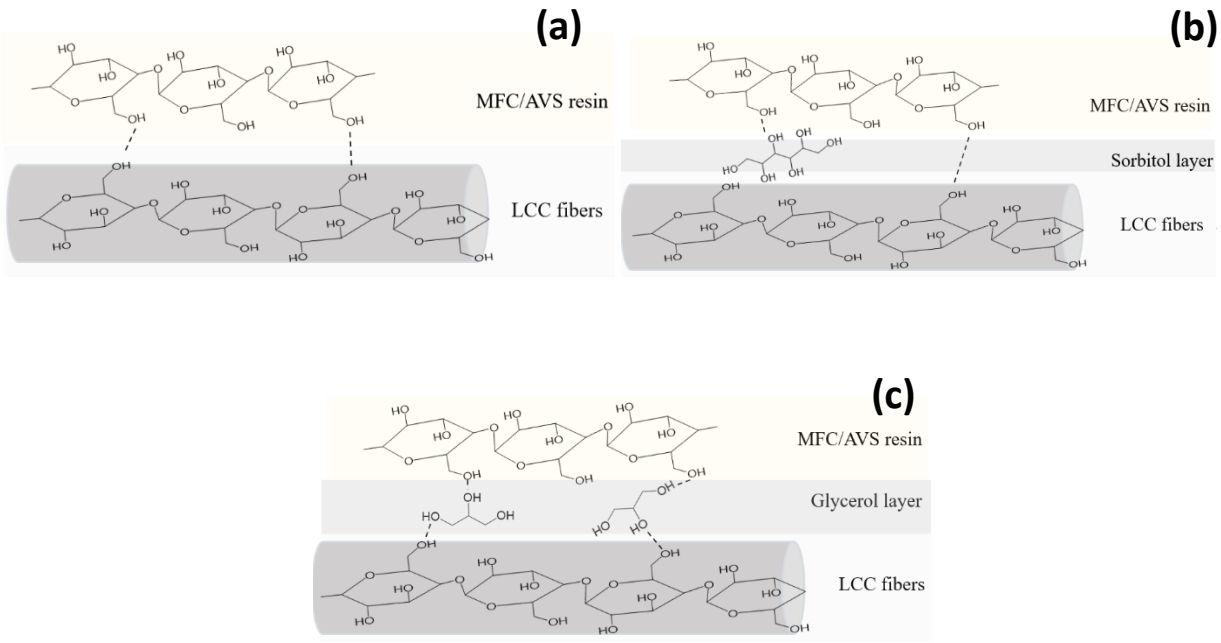

Fig. 23 Schematic illustration of the interfacial adhesion between LCC fibers and MFC/AVS resin with a) no plasticizer, b) 15% sorbitol and c) 15% glycerol

S-MFC/AVS was chosen as the resin to fabricate advanced green composites using control LCC and M-LCC fibers and their tensile properties were compared. Typical stress vs strain plots of LCC-S-MFC/AVS and M-LCC-S-MFC/AVS advanced green composites are shown in Figure 22 and tensile test data are presented in Table 9. A significantly higher Young's modulus of 19.5 GPa was obtained for M-LCC-S-MFC/AVS composites compared with 15.3 GPa obtained for LCC-S-MFC/AVS composites. This is over 27% enhancement in stiffness. The fracture stress of M-LCC-S-MFC/AVS composites (380.1 MPa) was also found to be 31% higher than LCC-S-MFC/AVS composites (289.9 MPa) having untreated LCC fibers. These results are as expected because of the much higher tensile properties of M-LCC fibers compared to LCC fibers as discussed earlier. Also, the fracture strain of the M-LCC fibers and untreated LCC are 5.6% and 6.4%, respectively, while the fracture strain values for M-LCC-S-MFC/AVS and LCC-S-MFC/AVS composites are

4.1% and 4.3%, respectively. Smaller difference Δ in strain values of single M-LCC fibers and their composites (Δ = 5.6% - 4.1% =1.5 %) compared with that of LCC fibers (Δ = 6.4% - 4.3% = 2.1%) suggests that there should be better bonding between S-MFC/AVS resin and M-LCC fibers than with LCC fibers. The enhanced M-LCC fiber/MFC/AVS interfacial adhesion can be expected to result in better stress transfer from broken to intact fibers thus better mechanical properties.[111]

4.7 Theoretical estimation of advanced green composites properties

The rule of mixture was used to estimate theoretical values for Young's modulus and the fracture stress of LCC-MFC/AVS composites. The theoretical fracture stress and Young's modulus values were calculated using equations:

$$\sigma_c = \sigma_f V_f + \sigma_m V_m$$

$$E_c = E_f V_f + E_m V_m$$

where *E* represents Young's modulus, σ represents fracture stress and V represents volume fraction and subscripts c, f and m stand for composite, fiber and matrix (resin), respectively.[53] Table 10 presents theoretical values of LCC and M-LCC fiber reinforced advanced green composites.

Table 10. Theoretical tensile test data of LCC-G-MFC/AVS and M-LCC-S-MFC/AVS advanced green composites

Composite	Fracture Stress (MPa)	Young's Modulus (GPa)	Fiber Volume Fraction
LCC-S-MFC/AVS theoretical	576.6	18.3	0.374
M-LCC-S-MFC/AVS theoretical	760.7	25.3	0.390

The calculated theoretical Young's modulus values for LCC-S-MFC/AVS and M-LCC-S-MFC/AVS advanced green composites are 18.3 GPa and 25.3 GPa, respectively. This is compared to the experimental Young's modulus values of 15.3 GPa and 19.5 GPa for the same composites. Although both experimental moduli are lower than the calculated values, they are not too far from the theoretical Young's modulus values. This indicates that the rule of mixture is a reasonable tool to predict Young's modulus of LCC composites. In any case, there are several reasons for obtaining lower experimental modulus values than theoretically predicted ones. The composites were hand laid and it was impossible to maintain perfect orientation of the fibers as it would be in an industrial situation. The resin penetration in between each filament may not be ideal. In addition, presence of any air bubbles or voids would also lower the values. The experimental fracture stress values of 289.75 MPa and 380.09 MPa for LCC-S-MFC/AVS and M-LCC-S-MFC/AVS composites, respectively, however, were much lower than the calculated fracture stress values of 576.55 MPa and 760.73 MPa, for the corresponding composites. The experimental values of ultimate stress are only around half of the prediction. This is a clear indication that many defects are present in the composites. As stated before, the main reasons for the lower experimental values include misalignment of LCC fibers embedded in the resin due to hand-processing, non-uniform resin penetration between LCC fibers and the introduction of defects, including voids and bubbles during hot-pressing. The nature of each type of defects and their individual contributions, however, are difficult to estimate. Also, since the composites failed at a lower strain levels (4~5.5%) than those of single LCC fibers (5.5%~6.5%), both LCC-S-MFC/AVS and LCC-G-MFC/AVS composites did not allow the LCC fibers to reach their full tensile potential. Several methods may be tried to avoid these errors, such as manually winding LCC yarns and immersing them in resin[11] or using pre-forming and prepreg sheet methods[112] and controlling the plasticizer amount to further

increase tensile strain while avoiding too much loss of interfacial adhesion. By using these methods, the final fracture strength should get closer to the theoretical value provided by rule of mixture.

4.8 Characterization of fracture surface topographies of advanced green composites

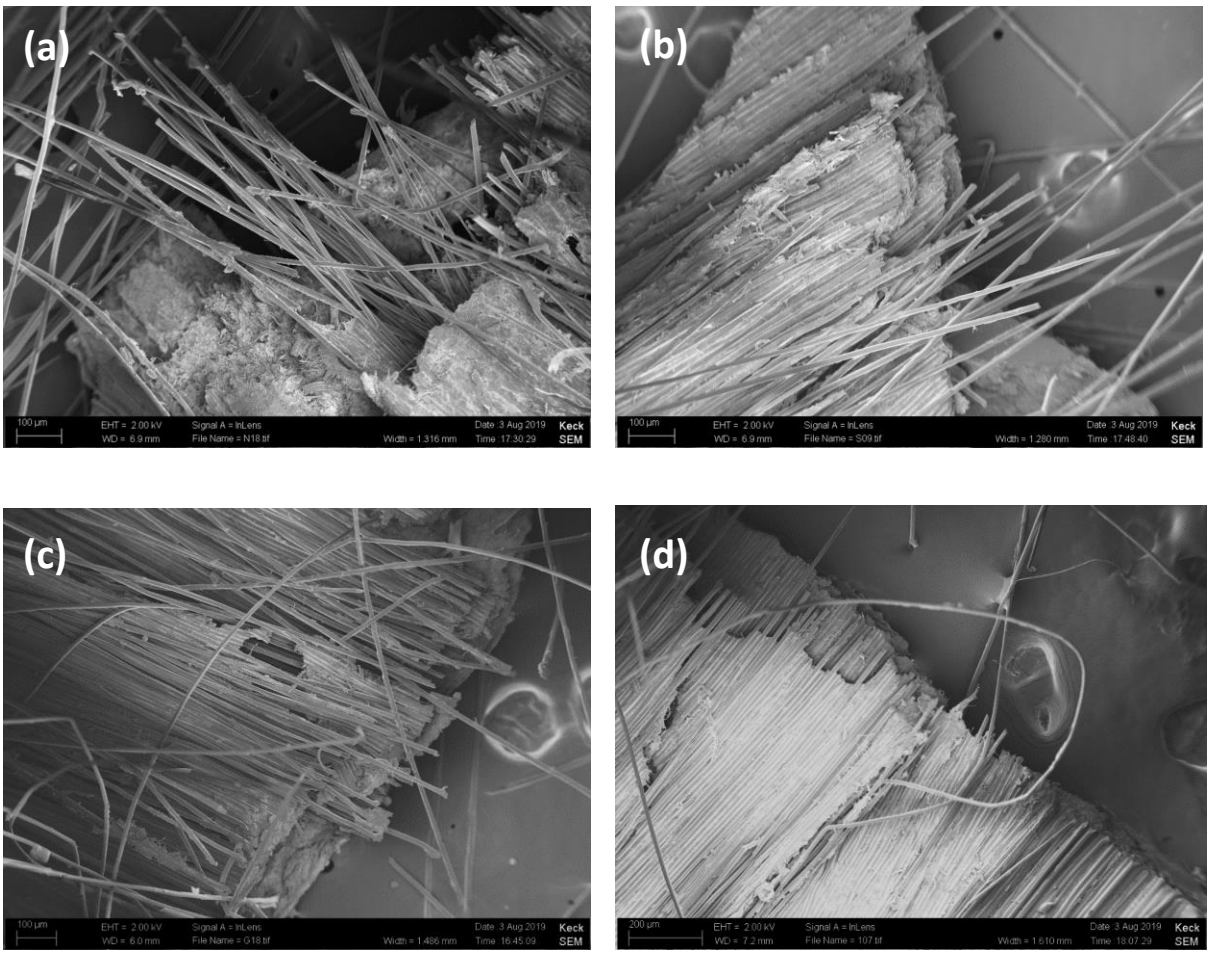

Fig. 24 SEM images of fracture surfaces of advanced green composites a) LCC-N-MFC/AVS; b) LCC-S-MFC/AVS; c) LCC-G-MFC/AVS; d) M-LCC-S-MFC/AVS

Typical SEM images of tensile fracture surfaces of LCC-N-MFC/AVS, LCC-S-MFC/AVS, LCC-G-MFC/AVS and M-LCC-S-MFC/AVS composites are presented in Figure 24. It is obvious that LCC fibers in N-MFC/AVS resin were most easily pulled out and showed the longest protruded lengths. The early fracture of the resin, which had fracture strain of lower than 3%, lowers the LCC fiber/resin interfacial shear strength as the resin cracks at different locations, leading to early failure of the composites and easy fiber pull-out.[6] However, after adding 15% sorbitol or glycerol, the fracture strains of the resins increased significantly. This led to much stronger interfacial bonding and less debonding occurred before fibers started to break.[6] Although some of the plasticizers can stay at the fiber/resin interface and reduce the interfacial shear strength, SEM pictures in Figures 24 (b) and (c) still show much shorter LCC fiber pull-out lengths than the resin without the plasticizer. The fracture surface of the M-LCC-S-MFC/AVS composite, shown in Figure 24 (d), exhibited the shortest pull-out lengths indicating the highest adhesion compared to other three composites. This further supports the hypothesis that higher interfacial bonding exists between the resin with M-LCC fibers compared to untreated LCC fibers. It is possible that after chemical and heat treatment, more hydroxyl groups are exposed on the LCC fiber surface which offer more hydrogen bonding sites with the AVS based resin, thus, providing better interfacial bonding.

CHAPTER 5: CONCLUSIONS

Fully biodegradable green composites were fabricated using non-edible starch extracted from avocado seed (AVS) and microfibrillated cellulose (MFC) or velvet leaf microfiber (VLF) and/or liquid crystalline cellulose (LCC) fibers. Avocado seed starch (AVS) was extracted by simple filtration technique and high purity starch (up to 84%) was obtained. To improve water resistance and mechanical properties of starch as resin, AVS was crosslinked using a green crosslinker, BTCA, to obtain thermoset starch having 3-D network structure. MFC or VLF were added to AVS to improve its fracture stress and Young's modulus. DMA, tensile tests and SEM analysis were conducted to characterize and compare the reinforced resin properties. The results indicated that both MFC and VLF do an excellent and almost equal job of reinforcing AVS resin. Both MFC and VLF were able to be dispersed in the AVS resin and provided significantly better water resistance or lower water absorption in the immersion test. Finally, liquid crystalline cellulose (LCC) fibers were combined with AVS resin to obtain advanced green composites with high tensile properties. LCC fibers were treated by potassium hydroxide solution as well as heat treatment to further enhance both molecular orientation and crystallinity of the fibers (M-LCC fibers). These treatments resulted in excellent enhancement in tensile properties of the M-LCC fibers. Tensile fracture stress and Young's modulus values of these advanced green composites were high and Young's modulus values were comparable to some conventional petroleum-derived engineering plastics. The type and amount of plasticizer used in AVS resin greatly affected its mechanical properties. Sorbitol, in general, resulted in better resin and composite properties than glycerol. Composites made with M-LCC fibers with 15% sorbitol-MFC/AVS resin were found to obtain a highest tensile strength of over 380 MPa and Young's modulus of 19.5 GPa with less than 40% volume fraction and in spite of using simple hand-processing techniques. Advanced green

composites reinforced with LCC fibers are not only fully biodegradable and sustainable but also exhibit high mechanical properties. They have excellent potential for use in many applications in the structural, automotive and engineering fields.

CHAPTER 6: FUTURE SUGGESTIONS

■ In the present study, avocado seed starch was used to make composites reinforced by microfibrillated cellulose and velvet leaf microfibers. Liquid crystalline cellulose fibers were used to make fully green advanced composites with high mechanical properties. The process of fabrication of composites could be made further green in several ways. First, the bleaching agent sodium chlorite used in this study is not environmental friendly. Further research should be carried by replacing sodium chlorite with hydrogen peroxide or other greener bleaching agents. The bleaching step may be even eliminated if single fibers could be separated by other methods.

■ The crosslinking catalyst, SHP, is not green because of the phosphorus it contains. Sodium propionate should be used in place of SHP to avoid introducing phosphorus.

■ Velvet leaf has shown excellent reinforcing capability and satisfies both requirement of good mechanical properties and uniform dispersity. Although not presented in this thesis, another type of fiber from hops stem (a waste), showed even larger aspect ratio when extracted by using the same process. The hops stem microfiber may have better reinforcing effect in starch-based composites. Future research may include this waste fiber for green composites.

■ Liquid crystalline cellulose fibers have been already modified using potassium hydroxide and sodium bisulfite and mechanical strength have been improved from 1500 MPa to nearly 2000 MPa.

While this research produced modified LCC fibers with strength higher than 1900 MPa, there is great scope to improve the strength further to over 2000 MPa if both the concentration and kind of treatment solution, loading weight and time are fully optimized. Different set of experiments may be designed to find the best treatment chemical and concentration and loading weight (tension) as well as treatment time and temperature. Also, the mechanism of strengthening during treatment is still not fully understood. It is believed that the lubrication of solution might help molecular orientation and increase crystallinity. Experiments could be carried out to examine the hypothesis.

■ The fabrication of LCC reinforced composites should be optimized. Misalignment and better penetration of LCC into matrix should be avoided as possible.

■ 15% of sorbitol was needed to ensure enough tensile strain of the resin. However, as seen from water absorption tests, high water absorption of 40~50% water sorption occurred for 15% sorbitol addition, which means that the starch-based composites are not applicable in humid environment. Hydrophobic treatment should be advantageous.

■ Biodegradability test for crosslinked starch films should be done to confirm how long it takes to fully biodegrade these green composites.

REFERENCES

1. Courtney, T. H. Mechanical Behavior of Materials, 2nd Edition. Waveland Press (2005). ISBN 1577664256.
2. Wang, R.-M., Zheng, S.-R. & Zheng, Y.-P. Polymer matrix composites and technology. Woodhead Publishing (2011).
3. Herakovich, C. T. Mechanics of Fibrous Composites. Wiley (1997).
4. Mallick, P. K. Fiber-Reinforced Composites: Materials, Manufacturing, and Design, Third edition. CRC Press (2007).
5. Ku, H., Wang, H., Pattarachaiyakoop, N. & Trada, M. A review on the tensile properties of natural fiber reinforced polymer composites. *Compos. Part B* **42**, 856–873 (2011).
6. Netravali, A. N., Henstenburg, R. B., Phoenix, S. L. & Schwartz, P. Interfacial shear strength studies using the single-filament-composite test. I: Experiments on graphite fibers in epoxy. *Polym. Compos.* **10**, 226–241 (1989).
7. 'Composites Industry Overview.' American Composites Manufactures Association, https://acmanet.org/composites-industry-overview/.
8. Yang, Y. Boom, R., Irion, B., Van Heerden, D-J., Kuiper, P. & De Wit, H. Recycling of composite materials. *Chem. Eng. Process. Process Intensif.* **51**, 53–68 (2012).
9. Netravali, A. N. & Chabba, S. Composites get greener. *Mater. Today* **6**, 22–29 (2003).
10. Gironès, J. Lopez, J. P., Mutjé, P. & Carvalho, A. Natural fiber-reinforced thermoplastic starch composites obtained by melt processing. *Compos. Sci. Technol.* **72**, 858–863 (2012).
11. Kim, J. T. & Netravali, A. N. Development of aligned-hemp yarn-reinforced green composites with soy protein resin: Effect of pH on mechanical and interfacial properties. *Compos. Sci. Technol.* **71**, 541–547 (2011).
12. Kim, J. T. & Netravali, A. N. Mercerization of sisal fibers: Effect of tension on mechanical properties of sisal fiber and fiber-reinforced composites. *Compos. Part A* **41**, 1245–1252 (2010).
13. Yan, L., Chouw, N. & Jayaraman, K. Flax fibre and its composites - A review. *Compos. Part B* **56**, 296–317 (2014).
14. Salim, M.S., Ariawan, D., Ahmad Rasyid, M. F., Ahmad Thirmizir, M. Z., Mat Taib, R. & Mohd. Ishak, Z. A. Effect of fibre surface treatment on interfacial and mechanical properties of non-woven kenaf fibre reinforced acrylic based polyester composites. *Polym. Compos.* **40**, E214–E226 (2019).
15. Dicker, M. P. M. Duckworth, P. F., Baker, A. B., Francois, G. & Hazzard, M. K. Green composites : A review of material attributes and complementary applications. *Compos. Part A* **56**, 280–289 (2014).

16. Sustainable Composites: Fibers, Resins and Applications, Netravali, A. N. and Pastore, C., (Eds.), DESTech Publications, Lancaster, PA (2014).

17. Advanced Green Composites, Netravali, A. N. (Ed.), Scrivener Publishing, Beverly, MA and Wiley, Hoboken, NJ (2018).

18. 'IAC FiberFrame™ Natural Fiber Sun Roof Frame Debuts on 2017 Mercedes-Benz E-Class.' International Automotive Components (2016). https://www.iacgroup.com/media/2016/04/04/iac-fiberframe-natural-fiber-sun-roof-frame-debuts-on-2017-mercedes-benz-e-class/.

19. Gáspár, M., Benko, Zs., Dogossy, G., Réczey, K. & Czigány, T. Reducing water absorption in compostable starch-based plastics. *Polym. Degrad. Stab.* **90**, 563–569 (2005).

20. Kahn, V. Characterization of Starch Isolated from Avocado. *J. Food Sci.* **52**, 1646–1648 (1987).

21. Ginting, M. H. S. Hasibuan, R., Lubis, M., Alanjani, F., Winoto, F. A. & Siregar, R. C. Utilization of Avocado Seeds as Bioplastic Films Filler Chitosan and Ethylene Glycol Plasticizer. *Asian J. Chem.* **30**, 1569–1573 (2018).

22. Chel-guerrero, L., Barbosa-martín, E., Martínez-antonio, A., González-mondragón, E. & Betancur-ancona, D. Some physicochemical and rheological properties of starch isolated from avocado seeds. *Int. J. Biol. Macromol.* **86**, 302–308 (2016).

23. Reddy, N. & Yang, Y. Characterizing natural cellulose fibers from velvet leaf (Abutilon theophrasti) stems. *Bioresour. Technol.* **99**, 2449–2454 (2008).

24. Patil, N. V & Netravali, A. N. Nonedible Starch Based "Green" Thermoset Resin Obtained via Esterification Using a Green Catalyst. *ACS Sustain. Chem. Eng.* **4**, 1756–1764 (2016).

25. Ghosh Dastidar, T. & Netravali, A. Cross-Linked Waxy Maize Starch-Based "Green" Composites. *ACS Sustain. Chem. Eng.* **1**, 1537–1544 (2013).

26. 'Bioplastics market data 2019', European Bioplastics. https://www.european-bioplastics.org.

27. Kalita, D. & Netravali, A. N. Thermoset Resin Based Fiber Reinforced Biocomposites:Recent Developments and Future Trends. Textile Finishing: Recent Developments and Future Trends. (2017)

28. Vilaseca, F., Mendez, J. A., Pèlach, A., Llop, M., Cañigueral, N., Gironès, J., Turon, X. & Mutjé, P. Composite materials derived from biodegradable starch polymer and jute strands. *Process Biochem.* **42**, 329–334 (2007).

29. Rico, M., Rodríguez-llamazares, S., Barral, L., Bouza, R. & Montero, B. Processing and characterization of polyols plasticized-starch reinforced with microcrystalline cellulose. *Carbohydr. Polym.* **149**, 83–93 (2016).

30. Hong, J., Zeng, X.-A., Brennan, C., Brennan, M. & Han, Z. Recent Advances in Techniques for Starch Esters and the Applications: A Review. *Foods* **5**, 1–15 (2016).

31. Meimoun, J. Wiatz, V., Saint-Loup, R., Parcq, J., Favrelle, A., Bonnet, F. & Zinck, P. Modification of starch by graft copolymerization. *Starch/Stärke* **70**, 1600351 (2018).

32. Jyothi, A. N., Moorthy, S. N. & Rajasekharan, K. N. Effect of cross-linking with epichlorohydrin on the properties of cassava (Manihot esculenta Crantz) starch. *Starch/Stärke* **58**, 292–299 (2006).

33. Hirsch, J. B. & Kokini, J. L. Understanding the mechanism of cross-linking agents (POCl3, STMP, and EPI) through swelling behavior and pasting properties of cross-linked waxy maize starches. *Cereal Chem.* **79**, 102–107 (2002).

34. Ghosh Dastidar, T.& Netravali, A. N. 'Green' crosslinking of native starches with malonic acid and their properties. *Carbohydr. Polym.* **90**, 1620–1628 (2012).

35. Reddy, N. & Yang, Y. Citric acid cross-linking of starch films. *Food Chem.* **118**, 702–711 (2010).

36. Xu, H., Canisag, H., Mu, B. & Yang, Y. Robust and Flexible Films from 100% Starch Cross-Linked by Biobased Disaccharide Derivative. *ACS Sustain. Chem. Eng.* **3**, 2631–2639 (2015).

37. Fringant, C., Moro, L. & Ave, L. Plasticized starch-cellulose interactions in polysaccharide composites. *Polym. (United Kingdom)* **42**, 6565–6572 (2001).

38. Sanyang, M. L., Sapuan, S. M., Jawaid, M., Ishak, M. R. & Sahari, J. Effect of plasticizer type and concentration on physical properties of biodegradable films based on sugar palm (arenga pinnata) starch for food packaging. *J. Food Sci. Technol.* **53**, 326–336 (2016).

39. Majdzadeh-Ardakani, K., Navarchian, A. H. & Sadeghi, F. Optimization of mechanical properties of thermoplastic starch/clay nanocomposites. *Carbohydr. Polym.* **79**, 547–554 (2010).

40. Huang, M., Yu, J. & Ma, X. Studies on the properties of Montmorillonite-reinforced thermoplastic starch composites. *Polym. (United Kingdom)* **45**, 7017–7023 (2004).

41. Sundum, T., Szécsényi, K. M. & Kaewtatip, K. Preparation and characterization of thermoplastic starch composites with fly ash modified by planetary ball milling. *Carbohydr. Polym.* **191**, 198–204 (2018).

42. Zhang, J. F. & Sun, X. Mechanical properties of poly(lactic acid)/starch composites compatibilized by maleic anhydride. *Biomacromolecules* **5**, 1446–1451 (2004).

43. Chang, P. R., Jian, R., Yu, J. & Ma, X. Fabrication and characterisation of chitosan nanoparticles / plasticised-starch composites. *Food Chem.* **120**, 736–740 (2010).

44. Ostafińska, A., Mikešová, J., Krejčíková, S., Nevoralová, M., Šturcová, A., Zhigunov, A. Michálková, D. & Šlouf, M. Thermoplastic starch composites with TiO2 particles: Preparation, morphology, rheology and mechanical properties. *Int. J. Biol. Macromol.* **101**, 273–282 (2017).

45. Satyanarayana, K. G., Arizaga, G. G. C. & Wypych, F. Biodegradable composites based on lignocellulosic fibers — An overview. *Prog. Polym. Sci.* **34**, 982–1021 (2009).

46. Peltola, H., Immonen, K., Johansson, L., Virkajärvi, J. & Sandquist, D. Influence of pulp bleaching and compatibilizer selection on performance of pulp fiber reinforced PLA biocomposites. *J. Appl. Polym. Sci.* **136**, 47955 (2019).

47. Hongsriphan, N. & Pinpueng, A. Properties of Agricultural Films Prepared from Biodegradable Poly (Butylene Succinate) Adding Natural Sorbent and Fertilizer. *J. Polym. Environ.* **27**, 434–443 (2019).

48. Patil, N. V. & Netravali, A. N. Enhancing Strength of Wool Fiber Using a Soy Flour Sugar-Based 'green' Cross-linker. *ACS Omega* **4**, 5392–5401 (2019).

49. Torres, F. G., Arroyo, O. H. & Gomez, C. Processing and mechanical properties of natural fiber reinforced thermoplastic starch biocomposites. *J. Thermoplast. Compos. Mater.* **20**, 207–223 (2007).

50. Versino, F. & García, M. A. Cassava (Manihot esculenta) starch films reinforced with natural fibrous filler. *Ind. Crops Prod.* **58**, 305–314 (2014).

51. Teixeira, E. D. M. Pasquini, D., Curvelo, A. A., Corradini, E., Belgacem, M. N. & Dufresne, A. Cassava bagasse cellulose nanofibrils reinforced thermoplastic cassava starch. *Carbohydr. Polym.* **78**, 422–431 (2009).

52. Patil, N. V & Netravali, A. N. Microfibrillated cellulose-reinforced nonedible starch-based thermoset biocomposites. *J. Appl. Polym. Sci.* **133**, 43803 (2016).

53. Patil, N. V, Rahman, M. M. & Netravali, A. N. " Green " Composites Using Bioresins from Agro-Wastes and Modified Sisal Fibers. *Polym. Compos.* **40**, 99–108 (2019).

54. Lubis, M., Gana, A., Maysarah, S., Ginting, M. H. . & Harahap, M. B. Production of bioplastic from jackfruit seed starch (Artocarpus heterophyllus) reinforced with microcrystalline cellulose from cocoa pod husk (Theobroma cacao L.) using glycerol as plasticizer. *IOP Conf. Ser. Mater. Sci. Eng.* **309**, 1 (2018).

55. Castaño. J., Rodríguez-Llamazares, S., Contreras, K., Carrasco, C., Pozo, C., Bouza, R., Franco, C. M. & Giraldo, D. Horse chestnut (Aesculus hippocastanum L .) starch : Basic physico-chemical characteristics and use as thermoplastic material. *Carbohydr. Polym.* **112**, 677–685 (2014).

56. Shepherd, J. S. California Avocado Society 1984 Yearbook. 68, 109 (1984).

57. Araújo, R. G. Rodriguez-Jasso, R. M. Ruiz, H. A. Pintado, M. M. E. & Aguilar, C. N. Avocado by-products: Nutritional and functional properties. *Trends Food Sci. Technol.* **80**, 51–60 (2018).

58. Tanpichai, S. Quero, F., Nogi, M., Yano, H., Lindström, T., Sampson, W. W. & Eichhorn, S. J. Effective young's modulus of bacterial and microfibrillated cellulose fibrils in fibrous networks. *Biomacromolecules* **13**, 1340–1349 (2012).

59. Joshi, S. V., Drzal, L. T., Mohanty, A. K. & Arora, S. Are natural fiber composites environmentally superior to glass fiber reinforced composites? *Compos. Part A* **35**, 371–376 (2004).

60. Mohanty, A. K., Vivekanandhan, S., Pin, J. M. & Misra, M. Composites from renewable and sustainable resources: Challenges and innovations. *Science* **362**, 536–542 (2018).

61. Pickering, K. L., Efendy, M. G. A. & Le, T. M. A review of recent developments in natural fibre composites and their mechanical performance. *Compos. Part A* **83**, 98–112 (2016).

62. Lodha, P. & Netravali, A. N. Characterization of interfacial and mechanical properties of " green " composites with soy protein isolate and ramie fiber. *J. Mater. Sci.* **37**, 3657–3665 (2002).

63. Brahmakumar, M., Pavithran, C. & Pillai, R. M. Coconut fibre reinforced polyethylene composites : effect of natural waxy surface layer of the fibre on fibre / matrix interfacial bonding and strength of composites. *Compos. Sci. Technol.* **65**, 563–569 (2005).

64. Luo, S. & Netravali, A. N. Mechanical and thermal properties of environment-friendly 'green' composites made from pineapple leaf fibers and poly(hydroxybutyrate-co-valerate) resin. *Polym. Compos.* **20**, 367–378 (1999).

65. Ashori, A. & Nourbakhsh, A. Bio-based composites from waste agricultural residues. *Waste Manag.* **30**, 680–684 (2010).

66. Abe, K., Iwamoto, S. & Yano, H. Obtaining Cellulose Nanofibers with a Uniform Width of 15 nm from Wood. *Biomacromolecules* **8**, 3276–3278 (2007).

67. Zhao, H. P., Feng, X. Q. & Gao, H. Ultrasonic technique for extracting nanofibers from nature materials. *Appl. Phys. Lett.* **90**, 2006–2008 (2007).

68. Herrick, F. W., Casebire, R. L., Hamilton, J. K. & Sandberg, K. R. Microfibrillated cellulose: morphology and accessibility. *J. Appl. Polym. Sci. Appl. Polym. Symp.* **37**, (1982).

69. Siró, I. & Plackett, D. Microfibrillated cellulose and new nanocomposite materials : a review. *Cellulose* **17**, 459–494 (2010).

70. Lu, P. & Hsieh, Y. Lo. Preparation and properties of cellulose nanocrystals: Rods, spheres, and network. *Carbohydr. Polym.* **82**, 329–336 (2010).

71. Afra, E., Yousefi, H., Mahdi, M. & Nishino, T. Comparative effect of mechanical beating and nanofibrillation of cellulose on paper properties made from bagasse and softwood pulps. *Carbohydr. Polym.* **97**, 725–730 (2013).

72. Khawas, P. & Deka, S. C. Isolation and characterization of cellulose nanofibers from culinary banana peel using high-intensity ultrasonication combined with chemical treatment. *Carbohydr. Polym.* **137**, 608–616 (2016).

73. Chen, W., Yu, H., Liu, Y., Hai, Y., Zhang, M. & Chen, P. Isolation and characterization of cellulose nanofibers from four plant cellulose fibers using a chemical-ultrasonic process. *Cellulose* **18**, 433–442 (2011).

74. Abe, K. & Yano, H. Comparison of the characteristics of cellulose microfibril aggregates of wood , rice straw and potato tuber. *Cellulose* **16**, 1017–1023 (2009).

75. Martins, I. M. G., Magina, S. P., Oliveira, L. Freire, C. S. R., Silvestre, A. J. D., Neto, C. P. & Gandini, A. New biocomposites based on thermoplastic starch and bacterial cellulose. *Compos. Sci. Technol.* **69**, 2163–2168 (2009).

76. Soykeabkaew, N., Laosat, N., Ngaokla, A., Yodsuwan, N. & Tunkasiri, T. Reinforcing potential of micro- and nano-sized fibers in the starch-based biocomposites. *Compos. Sci. Technol.* **72**, 845–852 (2012).

77. Jaafar, F. 'How Fiber Orientation and Configuration Contribute to Composite Performance?' The Fiber reinforced plastic & Composite Technology Resource Center. (2009) http://www.fibre-reinforced-plastic.com/2009/11/how-fibre-orientation-and-configuration.h.

78. Wollerdorfer, M. & Bader, H. Influence of natural fibres on the mechanical properties of biodegradable polymers. *Ind. Crops Prod.* **8**, 105–112 (1998).

79. Ma, X., Yu, J. & Kennedy, J. F. Studies on the properties of natural fibers-reinforced thermoplastic starch composites. *Carbohydr. Polym.* **62**, 19–24 (2005).

80. Qiu, K. & Netravali, A. N. Fabrication and characterization of biodegradable composites based on microfibrillated cellulose and polyvinyl alcohol. *Compos. Sci. Technol.* **72**, 1588–1594 (2012).

81. Huang, X. & Netravali, A. Biodegradable green composites made using bamboo micro/nano-fibrils and chemically modified soy protein resin. *Compos. Sci. Technol.* **69**, 1009–1015 (2009).

82. Rahman, M. M. & Netravali, A. N. polymeric resin from non-edible 'Jatropha curcas' seed waste after biodiesel production. *RSC Adv.* **6**, 47101–47111 (2016).

83. Rahman, M. M., Ho, K. & Netravali, A. N. Bio-based polymeric resin from agricultural waste, neem (azadirachta indica) seed cake, for green composites. *J. Appl. Polym. Sci.* **132**, 1–11 (2014).

84. Rahman, M. M. & Netravali, A. N. Green resin from forestry waste residue 'karanja (Pongamia pinnata) Seed cake' for biobased composite structures. *ACS Sustain. Chem. Eng.* **2**, 2318–2328 (2014).

85. Saito, T., Kimura, S., Nishiyama, Y. & Isogai, A. Cellulose nanofibers prepared by TEMPO-mediated oxidation of native cellulose. *Biomacromolecules* **8**, 2485–2491 (2007).

86. Agustin, M. B., Nakatsubo, F. & Yano, H. Improving the thermal stability of wood-based cellulose by esterification. *Carbohydr. Polym.* **192**, 28–36 (2018).

87. Wang, T. & Drzal, L. T. Cellulose-Nanofiber-Reinforced Poly(lactic acid) Composites Prepared by a Water-Based Approach. *ACS Appl. Mater. Interfaces* **4**, 5079–5085 (2012).

88. Suryanegara, L., Nakagaito, A. N. & Yano, H. The effect of crystallization of PLA on the thermal and mechanical properties of microfibrillated cellulose-reinforced PLA composites. *Compos. Sci. Technol.* **69**, 1187–1192 (2009).

89. Nakagaito, A. N., Fujimura, A., Sakai, T., Hama, Y. & Yano, H. Production of microfibrillated cellulose (MFC)-reinforced polylactic acid (PLA) nanocomposites from sheets obtained by a papermaking-like process. *Compos. Sci. Technol.* **69**, 1293–1297 (2009).

90. John, M. J. & Anandjiwala, R. D. Recent Developments in Chemical Modification and Characterization of Natural Fiber-Reinforced Composites. *Polym. Compos.* **29**, 187–207 (2008).

91. Sanyang, M. L. Sapuan, S. M., Jawaid, M., Ishak, M. R. & Sahari, J. Recent developments in sugar palm (Arenga pinnata) based biocomposites and their potential industrial applications: A review. *Renew. Sustain. Energy Rev.* **54**, 533–549 (2016).

92. Lodha, P. & Netravali, A. N. Characterization of phytagel® modified soy protein isolate resin and unidirectional flax yarn reinforced 'Green' composites. *Polym. Compos.* **26**, 647–659 (2005).

93. Fink, H. P., Weigel, P., Purz, H. J. & Ganster, J. Structure formation of regenerated cellulose materials from NMMO-solutions. *Prog. Polym. Sci.* **26**, 1473–1524 (2001).

94. Boerstoel, H., Maatman, H., Picken, S. ., Westerink, J. B. & Koenders, B. M. Liquid crystalline solutions of cellulose acetate in phosphoric acid. *Polymer (United Kingdom)* **42**, 7363–7369 (2001).

95. Borstoel, H. Liquid crystalline solutions of cellulose in phosphoric acid, PhD Thesis, Rijksuniversiteit, Groningen, The Netherlands (1998).

96. Netravali, A. N., Huang, X. & Mizuta, K. Advanced ' green ' composites. *Adv. Compos. Mater.* **16**, 269–282 (2007).

97. Kim, J. T. & Netravali, A. N. Fabrication of advanced 'green' composites using potassium hydroxide (KOH) treated liquid crystalline (LC) cellulose fibers. *J. Mater. Sci.* **48**, 3950–3957 (2013).

98. Rahman, M. M. & Netravali, A. N. Advanced Green composites using liquid crystalline cellulose fibers and waxy maize starch based resin. *Compos. Sci. Technol.* **162**, 110–116 (2018).

99. Ali, A., Yu, L., Liu, H., Khalid, S., Meng, L. & Chen, L. Preparation and characterization of starch-based composite films reinforced by corn / wheat hulls Preparation and characterization of starch-based composite films reinforced by corn and wheat hulls. *J. Appl. Polym. Sci.* (2017). doi:10.1002/app.45159

100. Takagi, H. & Ichihara, Y. E ffect of Fiber Length on Mechanical Properties of " Green " Composites Using a Starch-Based Resin and Short Bamboo Fibers. *JSME Int. J.* **47**, 551–555 (2004).

101. Mericer, C., Minelli, M. & Baschetti, M. G. Water sorption in microfibrillated cellulose (MFC): The effect of temperature and pretreatment. *Carbohydr. Polym.* **174**, 1201–1212 (2017).

102. Cao, X., Chen, Y., Chang, P. R., Muir, A. D. & Falk, G. Starch-based nanocomposites reinforced with flax cellulose nanocrystals. *Express Polym. Lett.* **2**, 502–510 (2008).

103. Liu, D., Zhong, T., Chang, P. R., Li, K. & Wu, Q. Bioresource Technology Starch composites reinforced by bamboo cellulosic crystals. *Bioresour. Technol.* **101**, 2529–2536 (2010).

104. Averous, L. & Boquillon, N. Biocomposites based on plasticized starch : thermal and mechanical behaviours. *Carbohydr. Polym.* **56**, 111–122 (2004).

105. Jacob, M., Francis, B. & Thomas, S. Dynamical Mechanical Analysis of Sisal / Oil Palm Hybrid Fiber-Reinforced Natural Rubber Composites. *Polym. Compos.* **27**, 671–680 (2006).

106. Lendvai, L., Karger-Kocsis, J., Kmetty, Á. & Drakopoulos, S. X. Production and characterization of microfibrillated cellulose-reinforced thermoplastic starch composites. *J. Appl. Polym. Sci.* **133**, 42397–42405 (2016).

107. Syverud, K. & Stenius, P. Strength and barrier properties of MFC films. *Cellulose* **16**, 75–85 (2009).

108. Wan, Y. Z., Luo, H., He, F., Liang, H., Huang, Y. & Li, X. L. Mechanical, moisture absorption, and biodegradation behaviours of bacterial cellulose fibre-reinforced starch biocomposites. *Compos. Sci. Technol.* **69**, 1212–1217 (2009).

109. Kaewtatip, K. & Thongmee, J. Preparation of thermoplastic starch/treated bagasse fiber compositesw. *Starch/Stärke* **66**, 724–728 (2014).

110. Boesel, L. F. Effect of plasticizers on the barrier and mechanical properties of biomimetic composites of chitosan and clay. *Carbohydr. Polym.* **115**, 356–363 (2015).

111. Ramli, W. M. A. W., Majid, M. S. A. & Sultan, M. T. H. The effect of nanomodified epoxy on the tensile and flexural properties of Napier fiber reinforced composites. *Polym. Compos.* 1–14, https://doi.org/10.1002/pc.25413 (2019).

112. Gomes, A., Matsuo, T., Goda, K. & Ohgi, J. Development and effect of alkali treatment on tensile properties of curaua fiber green composites. *Compos. Part A* **38**, 1811–1820 (2007).